



JET Simulations, Experiments and Theories

Modeling MHD jets and outflows*

Kanaris Tsinganos (tsingan@phys.uoa.gr)

Department of Physics, University of Athens, Greece



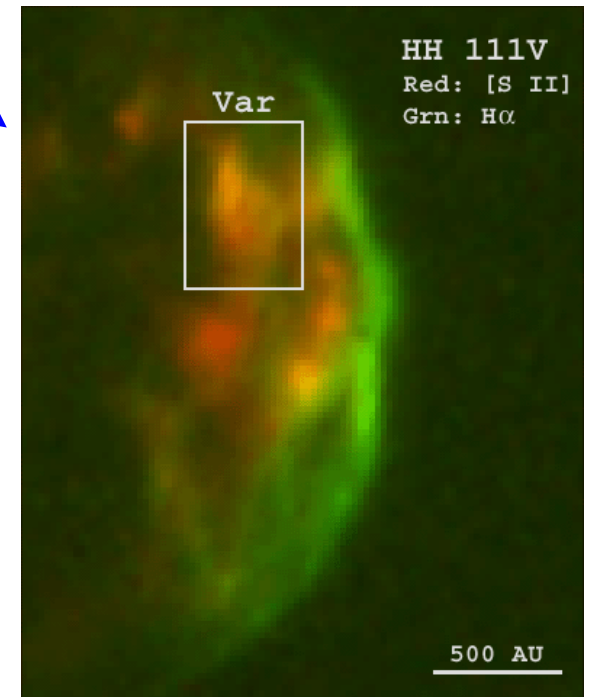
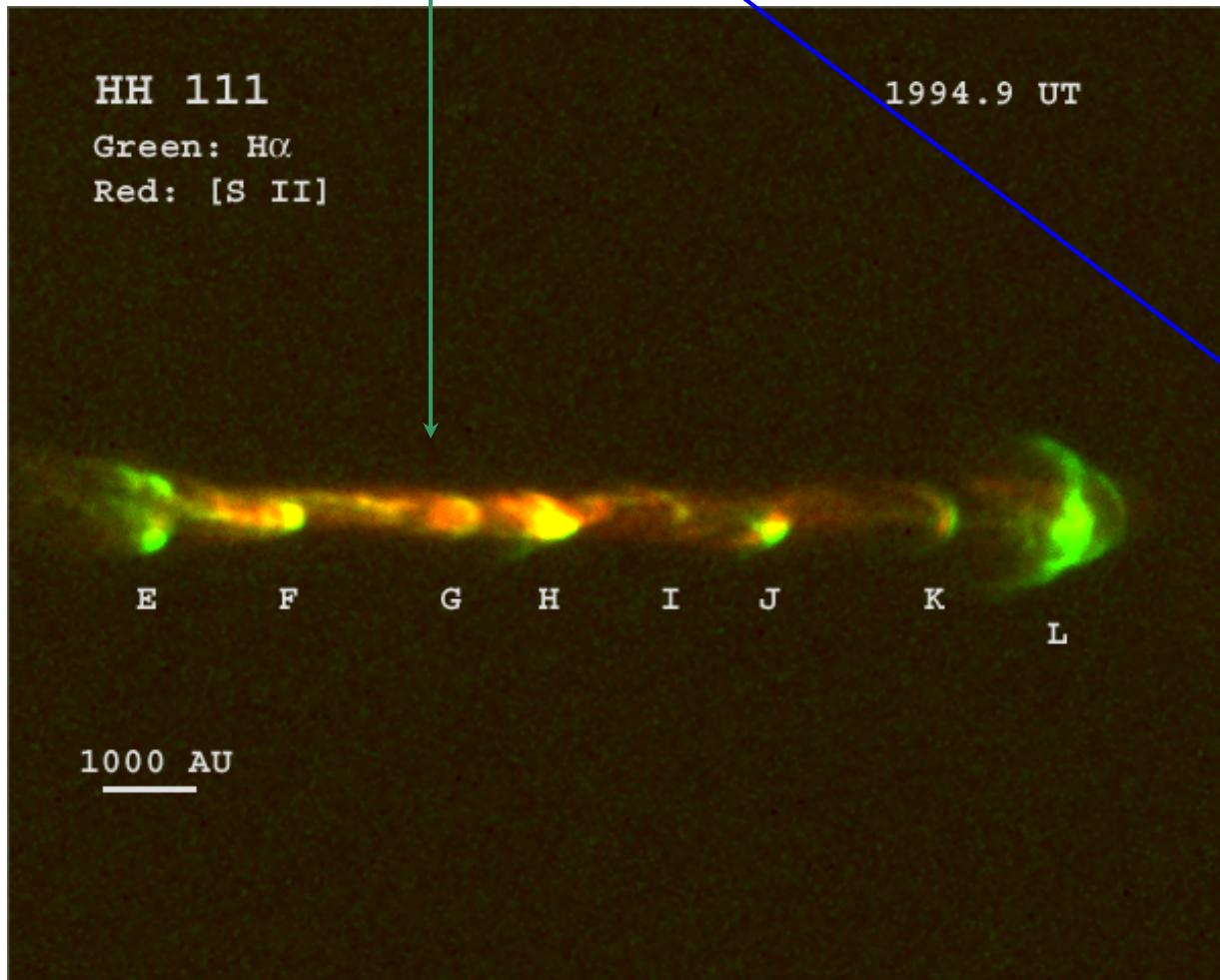
www.jetsets.org

**Various parts of this work have been performed in collaboration with :
Sergei Bogovalov (Moscow), Christophe Sauty (Paris), Silvano Massaglia, Edo
Trussoni and Titos Matsakos, (Torino), Nek Vlahakis (Athens)*

- Observations + Models
- Magnetic self-collimation
- **Analytical** solutions for **1-component** models :
 - Analytical Stellar Outflows (ASO)
 - Analytical Disk Outflows (ADO)
- **Numerical** solutions for **1-component** models :
Formation of a central jet in efficient magnetic rotators
- **Numerical** solutions for (non self-similar) **2-component** models :
Collimation of the stellar outflow by a surrounding disk-wind
- Results of **numerical** solutions for **2-component** models using
as initial conditions a combination of the ASO + ADO solutions
- Conclusions

Observations :Jets from YSO's

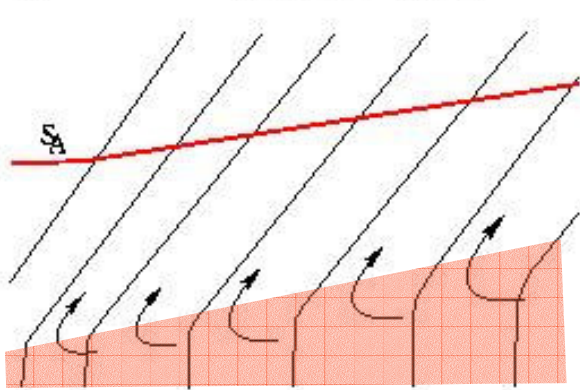
Propagation – bowshocks - source →



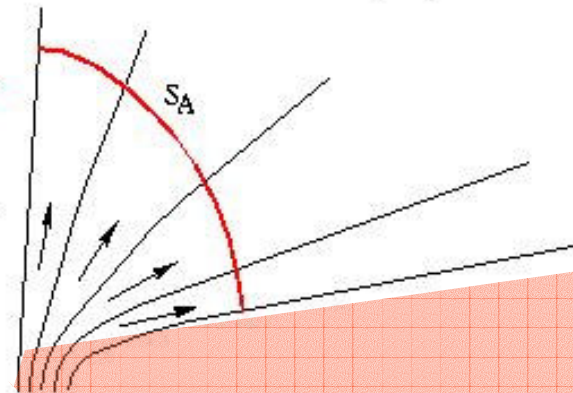
@ Pat Hartigan

The Origin of Jets

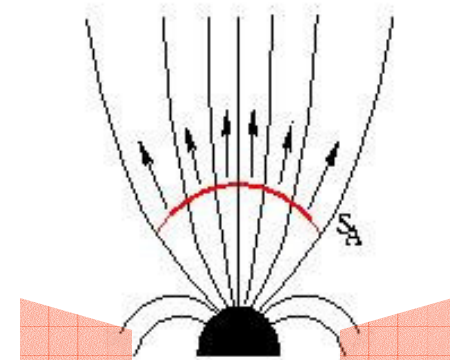
(a) Disc-wind: $r_e \gg r_i$



(b) X-wind: $r_e > r_i$



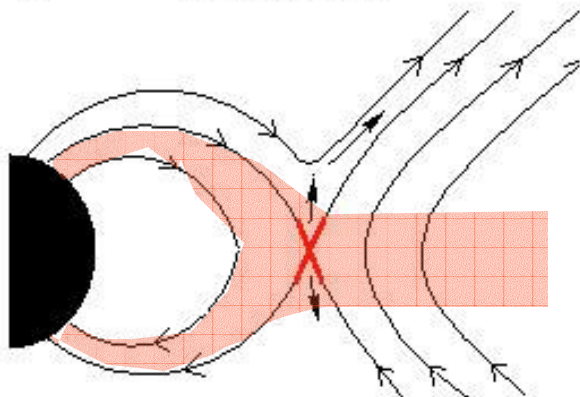
(c) Stellar wind



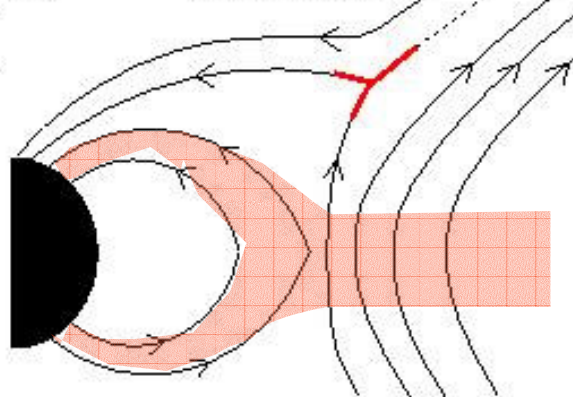
Steady ejection sites :

Extended disk-wind or inner disk wind (X-wind), or stellar wind

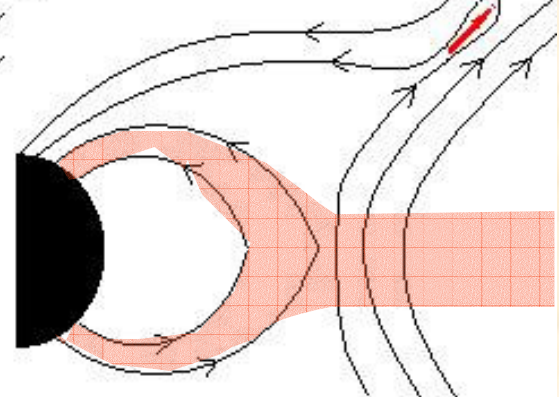
(d) X-type Interaction



(e) Y-type Interaction



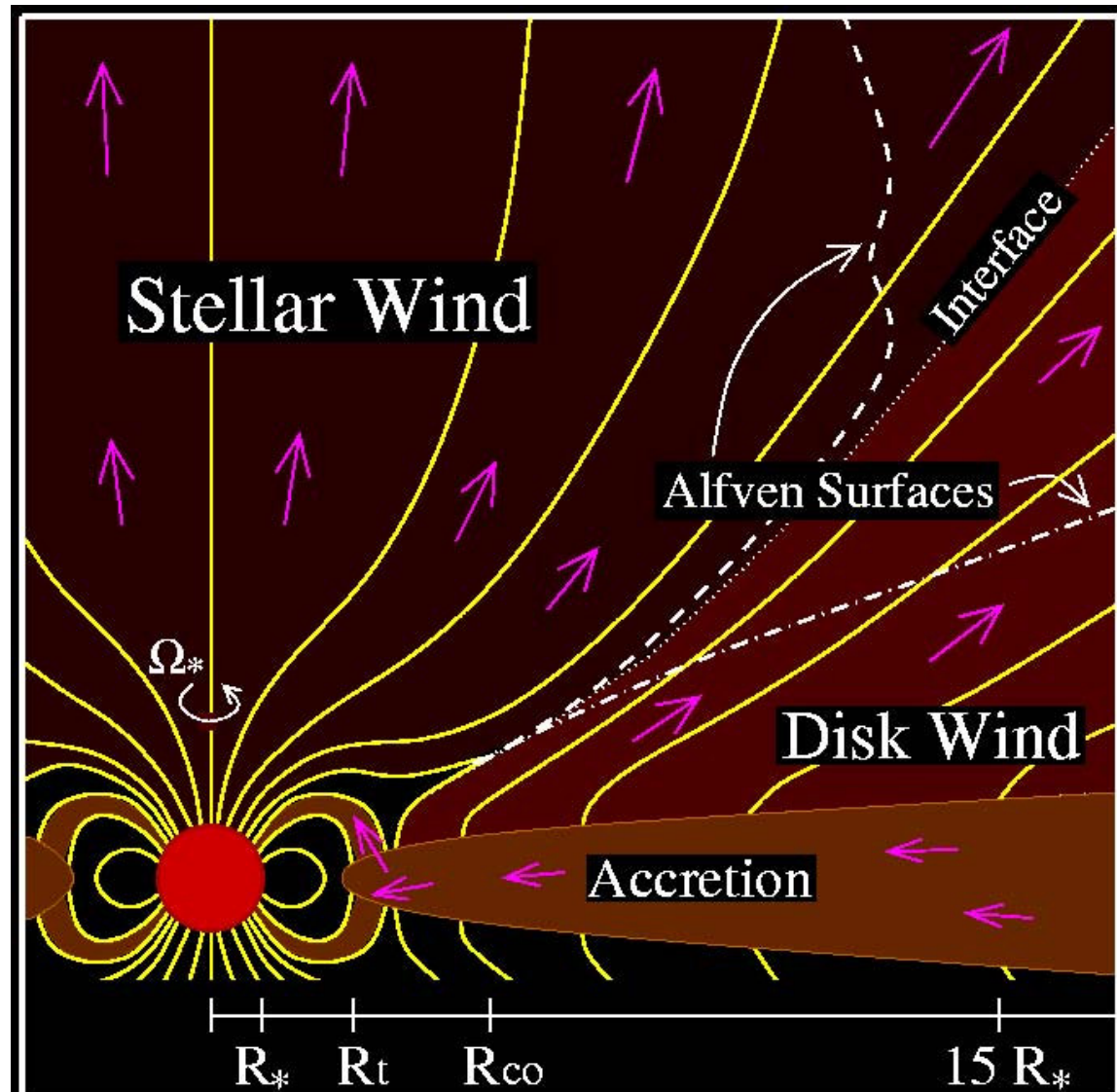
(f) CME-like mass loss



Unsteady ejection sites:

Re-X wind or CME-type ejections

Stellar wind vs. disk wind in spinning-down p^{*s}



Disk-locking seems problematic to explain the slow rotation of protostars

@ Matt & Pudritz, 2005



Spin-down of protostar via stellar wind :

JET Simulations, Experiments and Theories

Torque on star due to accretion of disk matter:

$$\tau_a \equiv \frac{dJ_a}{dt} = \dot{M}_a \sqrt{GM_* R_{trunc}}$$

Torque on star due to angular momentum lost in the wind :

$$\tau_w \equiv \frac{dJ_w}{dt} = -(2/3) \dot{M}_w \Omega_* R_*^2 (r_A/R_*)^2$$

Star rotates as a solid body at a rate which is a fraction f of break-up speed :

$$f = \Omega_* \sqrt{R_*^3/GM_*}$$

By equating $\tau_w = -\tau_a$, the equilibrium spin rate is,

$$f_{eq} \approx 0.1 \left(\frac{R_{trunc}/R_*}{2} \right)^{1/2} \times \left(\frac{r_A/R_*}{15} \right)^{-2} \times \left(\frac{\dot{M}_w/\dot{M}_a}{0.1} \right)^{-1}$$

- **Observations^(1,2)** : protostellar jet outflows contain two constituents, the dominance of which depends on the intrinsic physical properties of the system (protostellar object and disk)
(He line profiles indicate that stellar winds are present in at least 60% of CTTS)

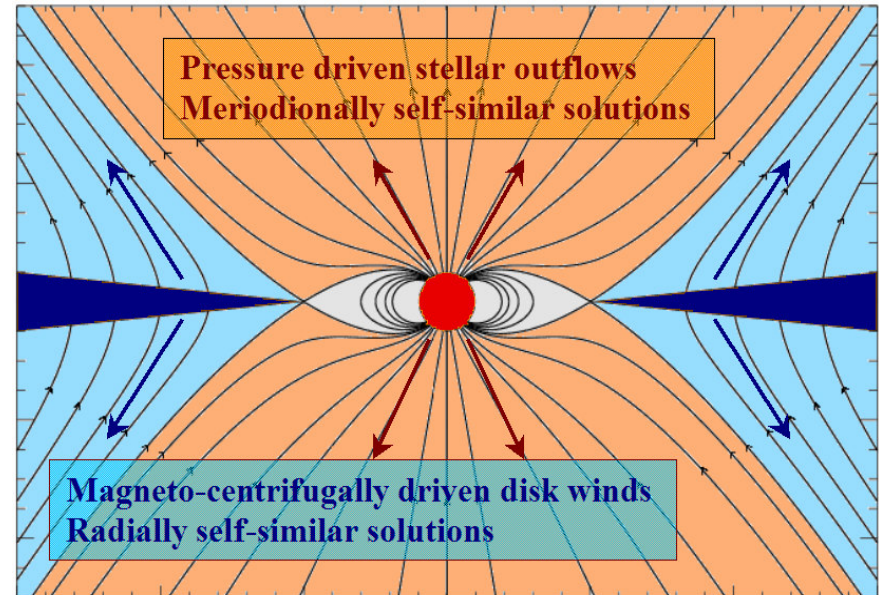
- Central protostar
- Surrounding disk

¹Edwards et al. (2006), ApJ, 646,319

²Kwan et al. (2007), ApJ, 657, 897

- **Theory⁽³⁾** : it is argued that jets from YSOs may consist of two components:
 - Inner pressure driven wind (non-collimated if the star is an inefficient magnetic rotator)
 - an outer magneto-centrifugally driven disk-wind providing most of the high mass loss rate observed.

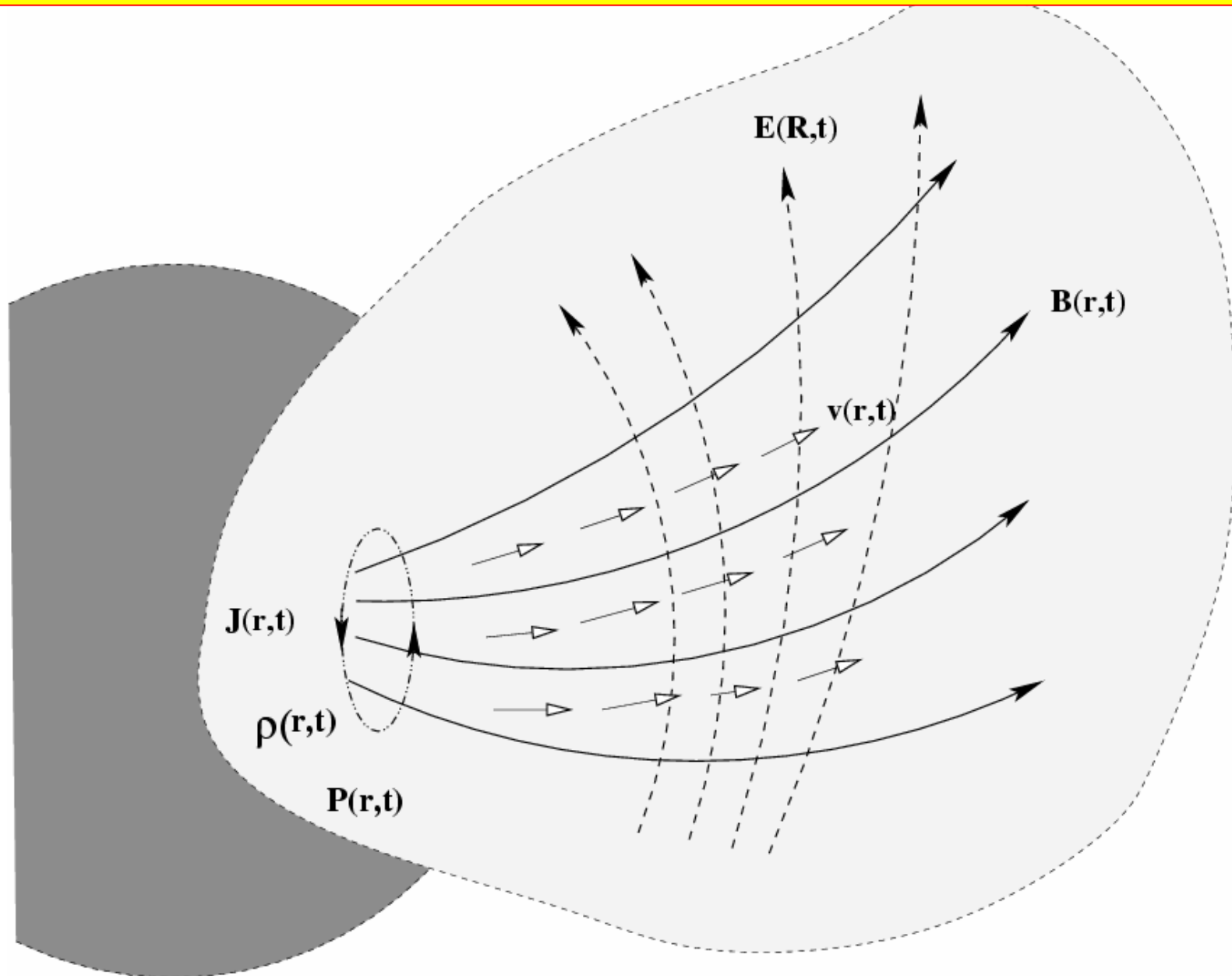
³Bogovalov & Tsinganos (2001), MNRAS, 325,249



Some “representative” studies in the past 50 years :

- Parker’s (1958 - 1960) classical description of the [HD Solar Wind](#)
- Weber & Davis (1967) description of an [equatorial magnetized stellar wind](#) with slow, Alfvén, fast [critical pts](#)
- Michel’s (1969) description of [relativistic](#) MHD stellar winds
- Blandford & Rees (1974), Lovelace (1976) [jets power double radio sources](#)
- Blandford & Payne’s (1982) description of radially self-similar MHD jets - “[bead on a rotating wire](#)” [analogy](#)
- Sakurai’s (1985) [numerical simulation](#) of MHD polytropic winds – first indications of [collimation](#)
- Uchida & Shibata’s (1985) simulations of the “[uncoiling spring mechanism](#)” for [launching](#) MHD jets
- Heyvaerts & Norman’s (1989, 2003) [asymptotic analyses](#) of rotating/magnetized outflows
- Sauty & Tsinganos (1994) description of meridionally [self-similar](#) MHD jets and [criterion for collimation](#)
- Vlahakis & Tsinganos (1998) [systematic construction of self-similar models](#) of MHD outflows
- Sauty, Trussoni, Tsinganos series of papers (1994 - 2005) on [analytical modelling self-similar](#) MHD outflows
- Ferreira, Casse, Keppens, Romanova (1997, 2002, 2004, 2006) [magnetized accretion-ejection structures](#)
- etc, etc.

Illustration of the interaction of magnetized plasmas



Theory : Basic (nonrelativistic) MHD equations

$$\vec{\nabla} \cdot \vec{\mathbf{B}} = 0, \quad \vec{\nabla} \cdot \vec{\mathbf{E}} = 4\pi\delta \approx 0,$$

$$\vec{\nabla} \times \vec{\mathbf{E}} = -\frac{1}{c} \frac{\partial \vec{\mathbf{B}}}{\partial t}, \quad \vec{\mathbf{E}} + \frac{\vec{\mathbf{V}} \times \vec{\mathbf{B}}}{c} = \frac{\vec{\mathbf{J}}}{\sigma} \approx 0, \quad \text{Maxwell}$$

$$\vec{\nabla} \times \vec{\mathbf{B}} = \frac{4\pi}{c} \vec{\mathbf{J}} + \frac{1}{c} \frac{\partial \vec{\mathbf{E}}}{\partial t} \approx \frac{4\pi}{c} \vec{\mathbf{J}},$$

$$\rho \frac{\partial \vec{\mathbf{V}}}{\partial t} + (\rho \vec{\mathbf{V}} \cdot \vec{\nabla}) \vec{\mathbf{V}} = -\vec{\nabla} P + \frac{\vec{\mathbf{J}} \times \vec{\mathbf{B}}}{c} - \rho \vec{\mathbf{G}}, \quad \text{Newton}$$

$$\vec{\nabla} \cdot \rho \vec{\mathbf{V}} + \frac{\partial \rho}{\partial t} = 0, \quad \text{mass conservation}$$

$$\rho \left[P \frac{d}{dt} \left(\frac{1}{\rho} \right) + \frac{d}{dt} \left(\frac{P}{\rho(\Gamma - 1)} \right) \right] = \rho \frac{\partial h}{\partial t} - \frac{\partial P}{\partial t} + \rho \vec{\mathbf{V}} \cdot \left[\nabla h - \frac{\nabla P}{\rho} \right] = q.$$

$\vec{\mathbf{V}}(x_1, x_2, x_3, t)$: Bulk Flow Speed of Plasma

$\vec{\mathbf{B}}(x_1, x_2, x_3, t)$: Magnetic Field in Plasma

$\vec{\mathbf{J}}(x_1, x_2, x_3, t)$: Electric Current Density in Plasma

$\vec{\mathbf{G}}(x_1, x_2, x_3)$: External (gravitational) Field in Plasma

$\rho(x_1, x_2, x_3, t)$: Plasma Density

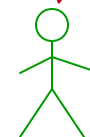
$P(x_1, x_2, x_3, t)$: Plasma Pressure

$h(x_1, x_2, x_3, t)$: Enthalpy ($= \frac{\Gamma}{\Gamma-1} \frac{P}{\rho}$)

$q(x_1, x_2, x_3, t)$: Volumetric Rate of Energy Addition in System

Question:

How can we “extract” from the general set of these MHD Eqs. the description of a magnetized outflow (jet or wind) ??



- I. Steady models

Advantages:

- analytical treatment
- parametric study
- physical picture
- cheap method

Difficulties:

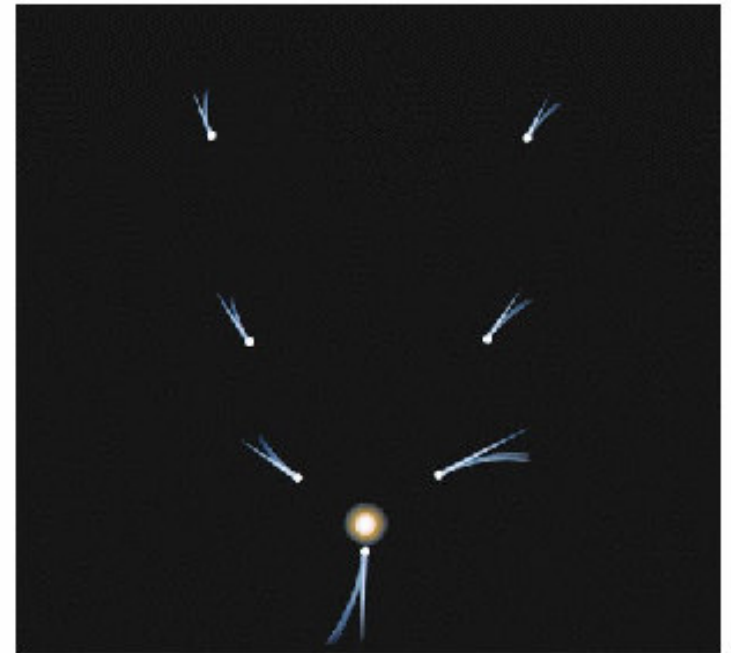
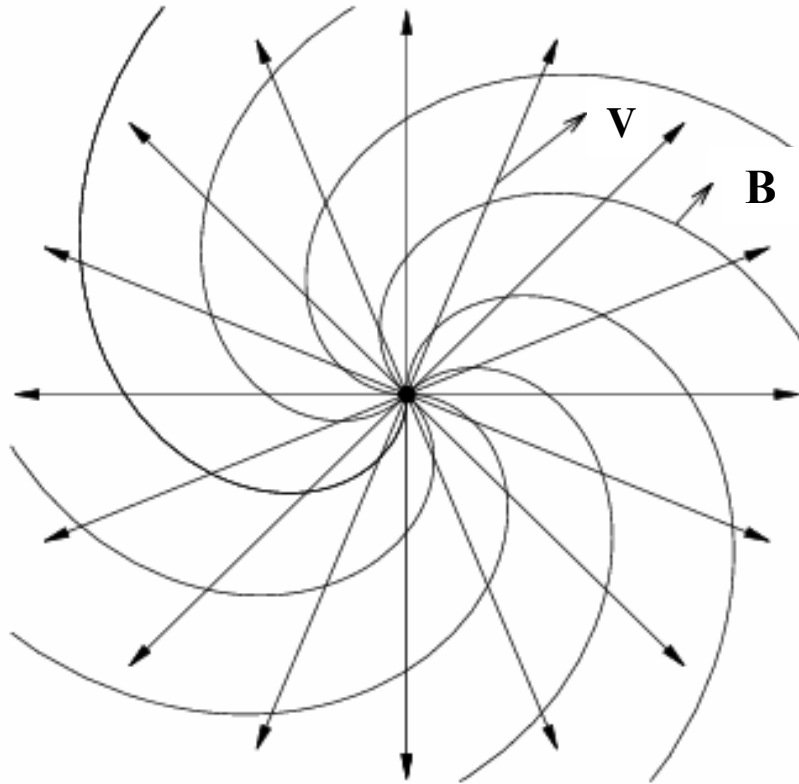
- Nonlinearity of MHD set !
- 2-dimensionality - PDEs !
- Causality - unknown critical surfaces !

- II. Time-dependent models

- (No-analytical treatment)
- temporal evolution
- nonideal MHD effects
- (expensive method)

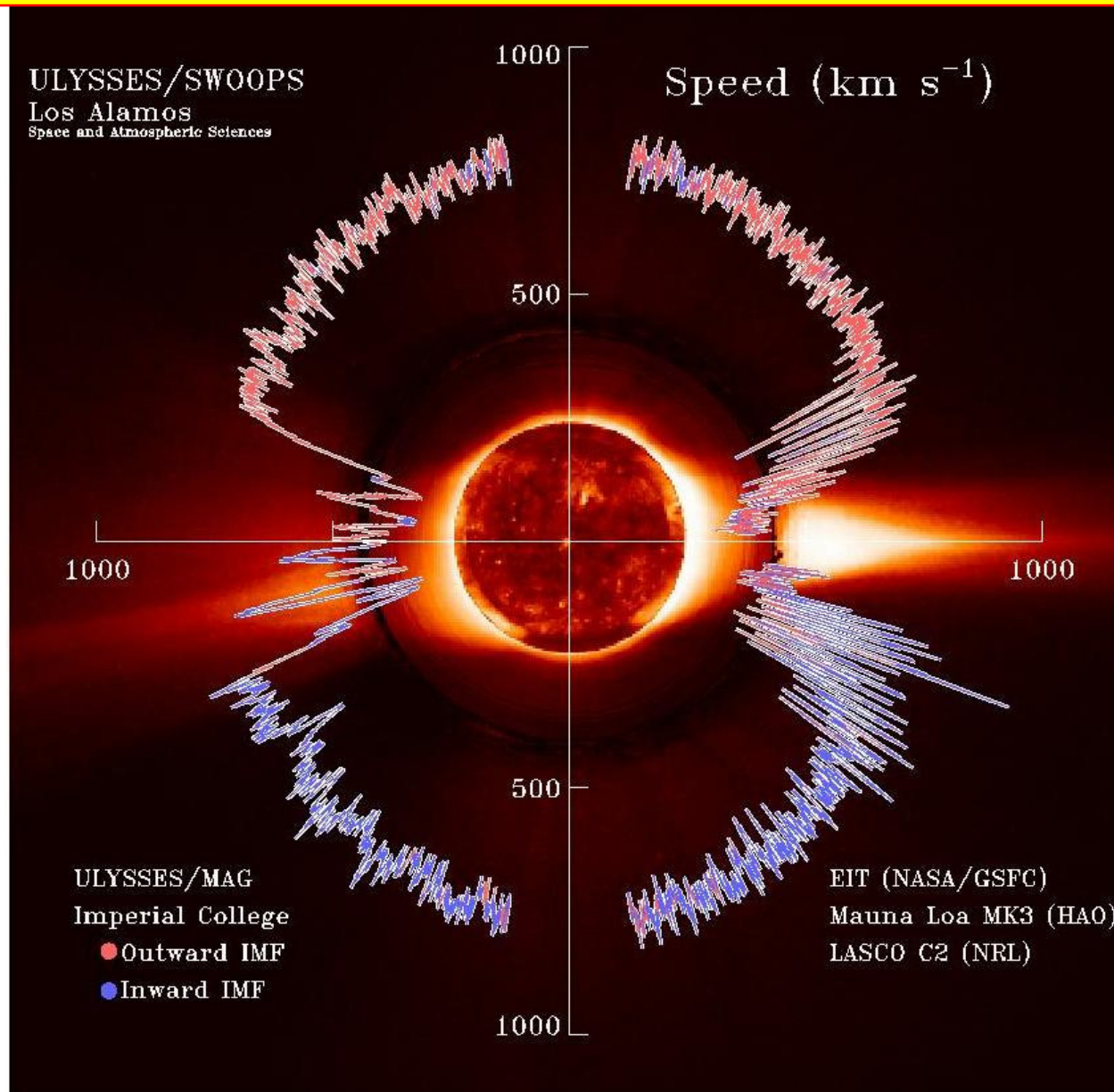
- 3D MHD code with magnetic flux conservation !
- large grid space - large lengths of jets !
- correct boundary conds - boundary effects !

Ia) 1D-HD : The classical Parker wind

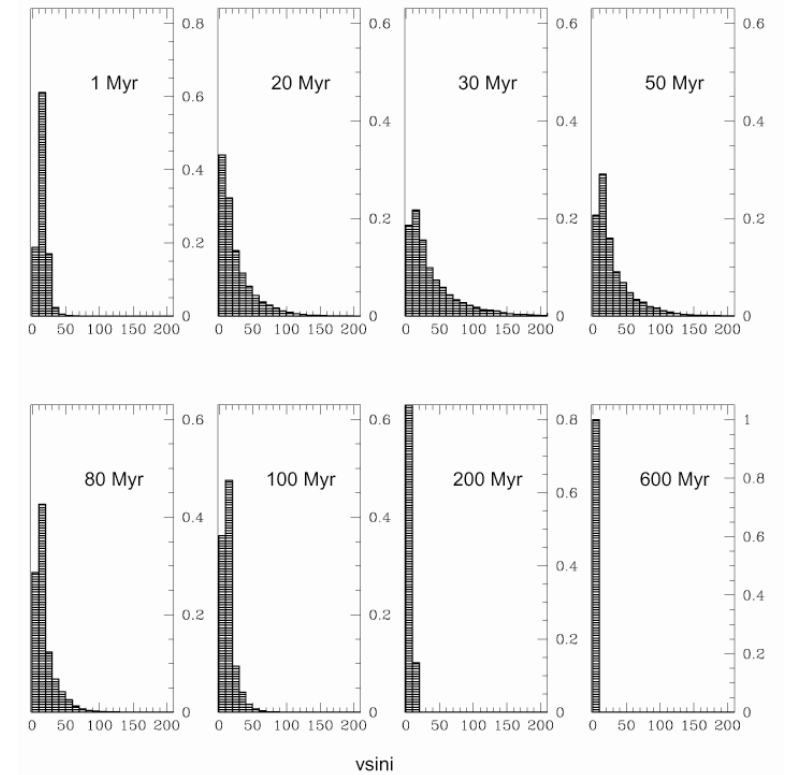
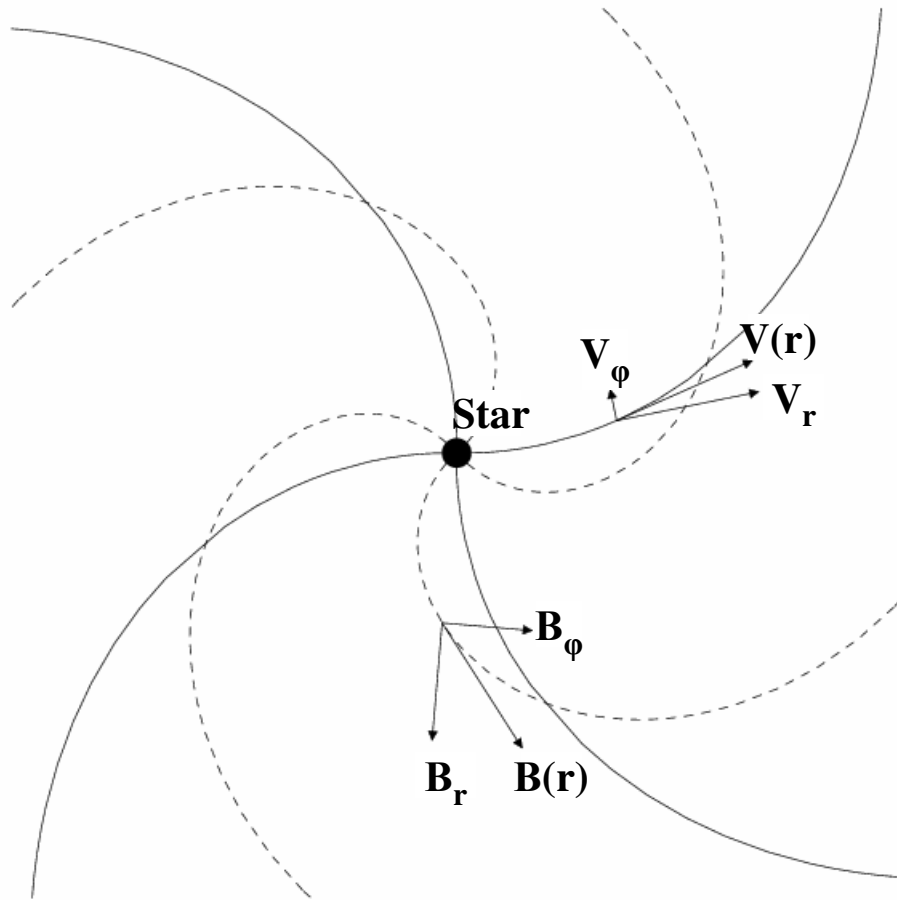


Ulysses *in situ* measurement of solar wind speed

[Sauty et al, AA, 432, 687, 2005]:

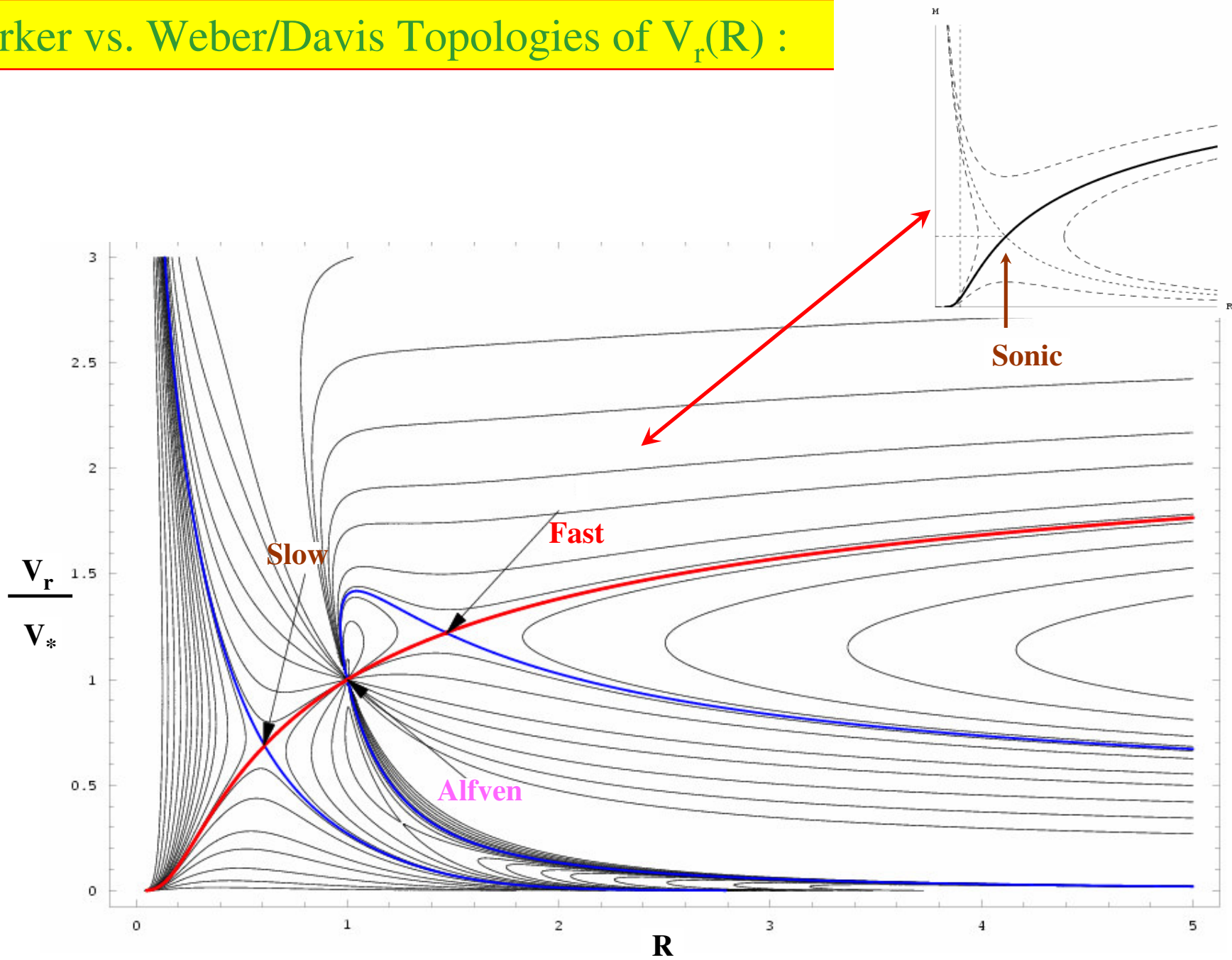


Ib) 1D-MHD: The Weber-Davis magnetized wind



Distribution of $V \sin i$ for $1M_\odot$ stars of different ages (Bouvier, Forestini & Alain 1997)

Parker vs. Weber/Davis Topologies of $V_r(R)$:



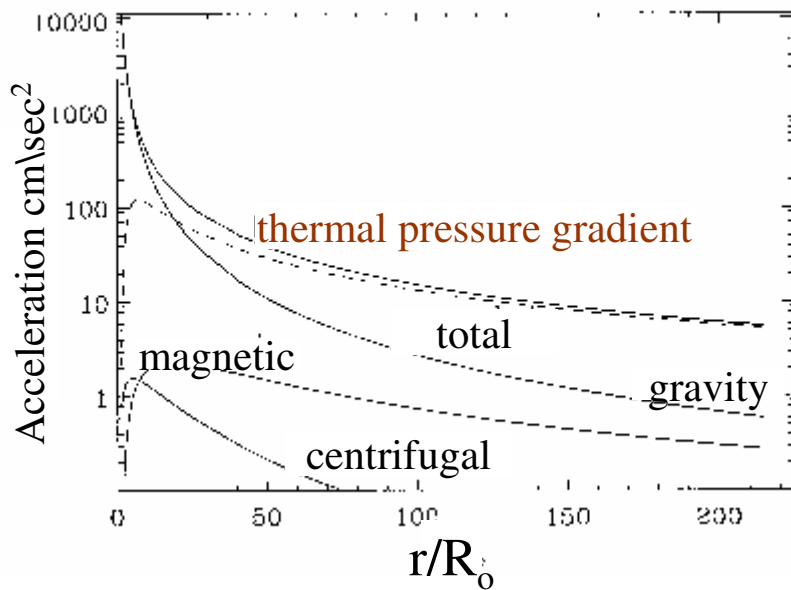
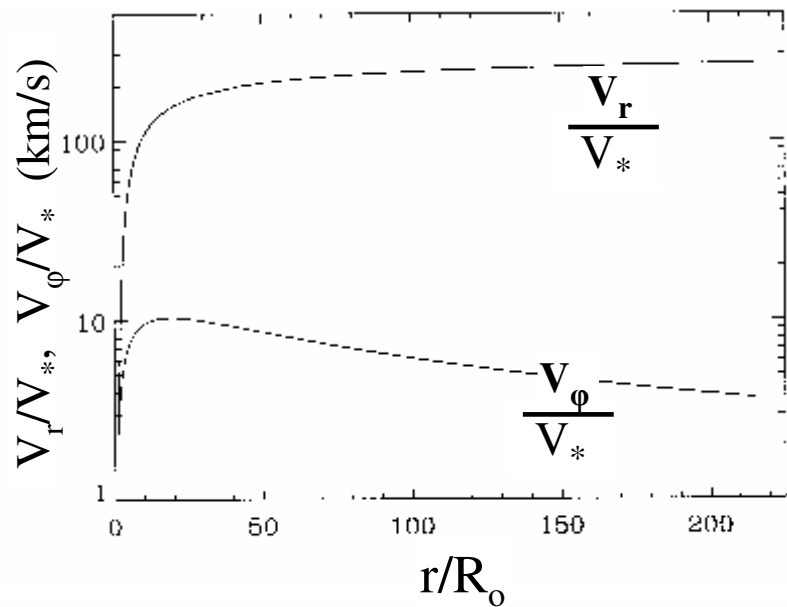
Slow and Fast magnetic rotators :

$$\mathcal{E} = \frac{1}{2}V^2 + h - \frac{GM}{r} - \frac{rB_\phi\Omega}{\Psi_A} = \underbrace{\frac{1}{2}V_o^2 + h_o - \frac{GM}{r_o}}_{\mathcal{E}_o} - \underbrace{\frac{r_o B_\phi^2 \Omega}{\Psi_A}}_{\Omega L}, \quad \mathcal{E} \simeq \mathcal{E}_o + \Omega L,$$

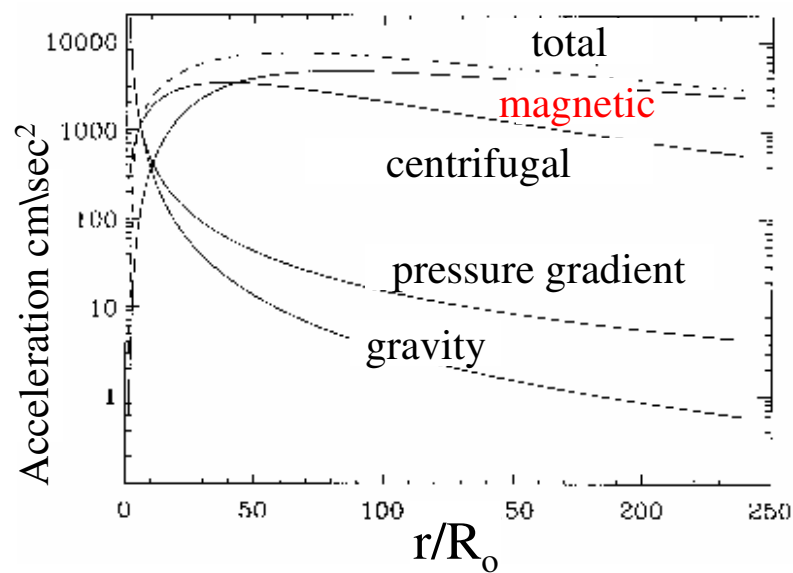
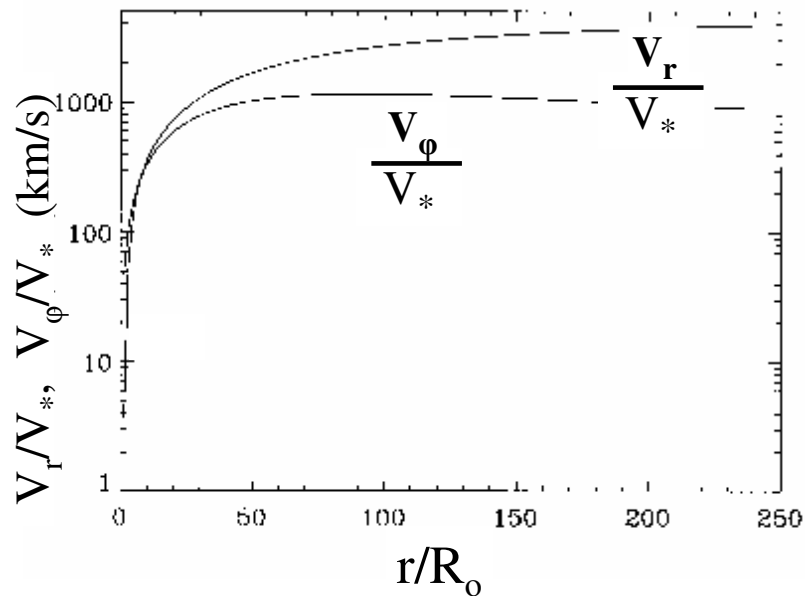
where \mathcal{E}_o is the energy of the thermally driven Parker wind and ΩL the Poynting energy of the magnetic rotator. Depending on which of these two terms dominates we have two possibilities:

1. $\mathcal{E}_o \gg \Omega L$: Slow magnetic rotator. In this case we have a thermally driven Parker wind
2. $\mathcal{E}_o \ll \Omega L$: Fast magnetic rotator. In this case we have a magnetorotationally driven wind

Slow magnetic rotator (our Sun)



Fast magnetic rotator (YSO)



II. 2-D MHD plasma outflows: the issue of collimation

- a) Time-independent (steady) outflows
 - i) meridionally selfsimilar
 - ii) radially selfsimilar

- b) Time-dependent plasma outflows

a). 2-D Time-independent (steady) studies - some general conclusions :

- Classes of analytical solutions via a nonlinear separation of the variables (Vlahakis+Tsinganos, 298, 777, 1998)
- Critical points, characteristics and the problem of causality (Tsinganos et al, MNRAS 283, 811, 1996, Vlahakis et al, MNRAS, 318, 417, 2000)
- Classification of observed outflows in terms of efficiency of magnetic rotator (Sauty et al, 348, 327, 1999, Sauty et al, AA, 389, 1068, 2002)
- Topological stability of collimated outflows (Vlahakis + Tsinganos, MNRAS, 292, 591, 1997)
- etc, etc.

Reduced Form of MHD Equations for *Axisymmetric Plasma States*

Magnetic and mass flux functions:

$$\text{Magnetic Flux: } F = \iint_S \vec{\mathbf{B}}_p \cdot d\vec{\mathbf{S}} = 2\pi A, \quad \vec{\mathbf{B}}_p = \vec{\nabla} \times \left(\frac{A}{\varpi} \hat{\phi} \right), \quad \leftarrow \boxed{\text{div.}\mathbf{B} = 0}$$

$$\text{Mass Flux: } \dot{M} = \iint_S \rho \vec{\mathbf{V}}_p \cdot d\vec{\mathbf{S}} = \frac{\Psi}{2}, \quad \rho \vec{\mathbf{V}}_p = \vec{\nabla} \times \left(\frac{\Psi}{4\pi\varpi} \hat{\phi} \right) \quad \leftarrow \boxed{\text{div.}\rho\mathbf{V}_p = 0}$$

\Rightarrow 4 MHD Integrals:

$$\text{Streamfunction } \Psi(A) : \quad \mathbf{V}_p = \frac{\Psi_A}{4\pi\rho} \mathbf{B}_p,$$

$$\text{Angular Momentum } L(A) : \quad L(A) = \varpi \left(V_\varphi - \frac{B_\varphi}{\Psi_A} \right),$$

$$\text{Corotation Frequency } \Omega(A) : \quad V_\varphi - \Omega\varpi = \frac{\Psi_A}{4\pi\rho} B_\varphi,$$

$$\text{Total Energy } E(A) : \quad \frac{1}{2} |\vec{\mathbf{V}}|^2 + \frac{\gamma}{\gamma-1} \frac{P}{\rho} + \Phi - \frac{\Omega}{\Psi_A} \varpi B_\varphi = E(A),$$

\Rightarrow Transfield equation for magnetic flux function $A(z, \varphi)$:

[Tsinganos, ApJ, 252, 775, 1982]

$$\left[1 - \frac{\Psi_A^2}{4\pi\rho} \right] \left[\vec{\nabla} \cdot \left(\frac{\vec{\nabla} A}{\varpi^2} \right) \right] - \Psi_A \left[\frac{\vec{\nabla} A}{\varpi^2} \right] \cdot \left[\vec{\nabla} \left(\frac{\Psi_A}{4\pi\rho} \right) \right] + F(A, \Psi, L, \Omega, \rho) = 0$$

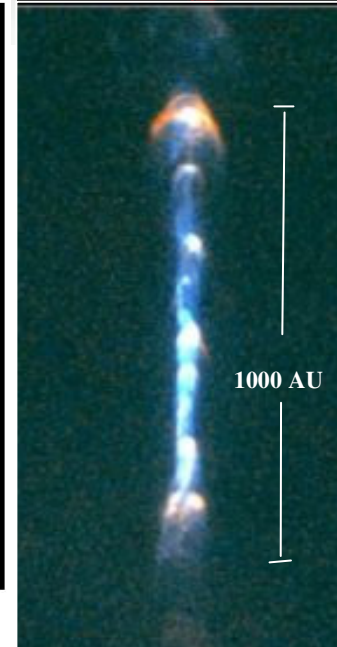
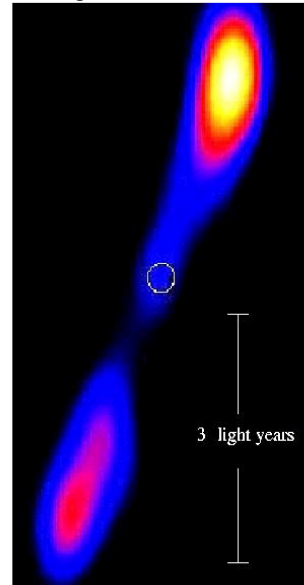
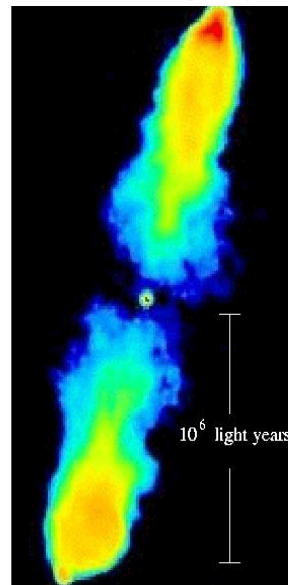
Analytical Solutions: Self-similarity



Quasar/radio galaxy

Microquasar 1E1740.7-2942

Protostellar jet HH 111



The problem of a **systematic** construction of exact models for astrophysical MHD plasma flows

Main assumptions for getting analytical solutions

1. *Ideal* MHD.
2. *Symmetric* outflow configurations, $\partial_3 = 0$, in system (x_1, x_2, x_3) e.g., axisymmetric, or translationally symmetric.
3. *Natural* variables are poloidal Alfvén number and magnetic flux function $(M, A) \implies$ switch from (x_1, x_2) to (M, A) .
4. Consider Alfvén number $M(x_1, x_2)$ and cross-section of outflow tube $G(x_1, x_2)$ as functions of a single variable χ :

$$M = M(\chi), G = G(\chi)$$

I. In spherical coordinates $(x_1 = r, x_2 = \theta,)$ this unifying scheme contains two large groups of exact MHD outflow models:

(α) $\chi = \theta \longrightarrow$ *radially* self-similar models with *conical* critical surfaces. Prototype is the Blandford & Payne¹ (1982) model :

$$A(r, \theta) = g(\theta)r^x \text{ and } x = 3/4.$$

(β) $\chi = r \longrightarrow$ *meridionally* self-similar models with *spherical* critical surfaces. Prototype is the Sauty & Tsinganos² (1994) model :

$$A(r, \theta) = f(r)\sin^{2\epsilon}\theta \text{ and } \epsilon=1.$$

II. In orthogonal coordinates $(x_1 = x, x_2 = y,)$ this unifying scheme contains the group of *planarly* self-similar MHD models. Prototype is the Petrie et al³ (2002) model :

$$A = G(x)e^{-z/H}$$

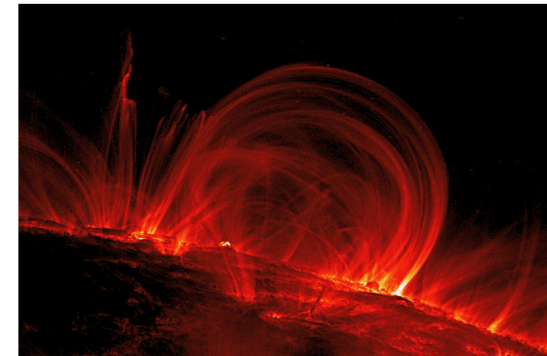
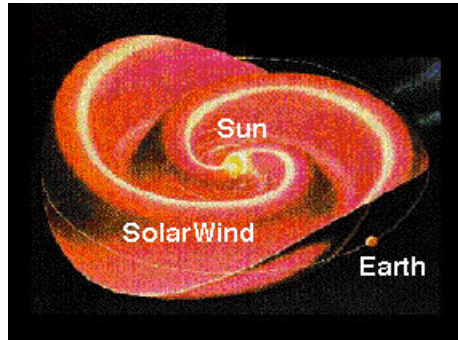
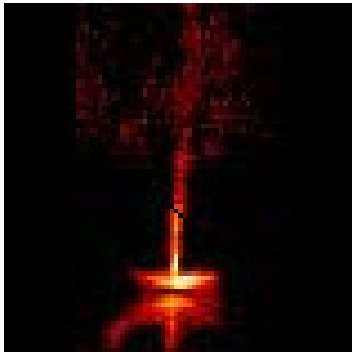
[†]Vlahakis & Tsinganos 1998, MNRAS, **298**, 777

¹Blandford & Payne 1982, MNRAS, **199**, 883

²Sauty & Tsinganos 1994, A&A, **287**, 893

³Petrie, Vlahakis & Tsinganos 2001, A&A, **382**, 1081

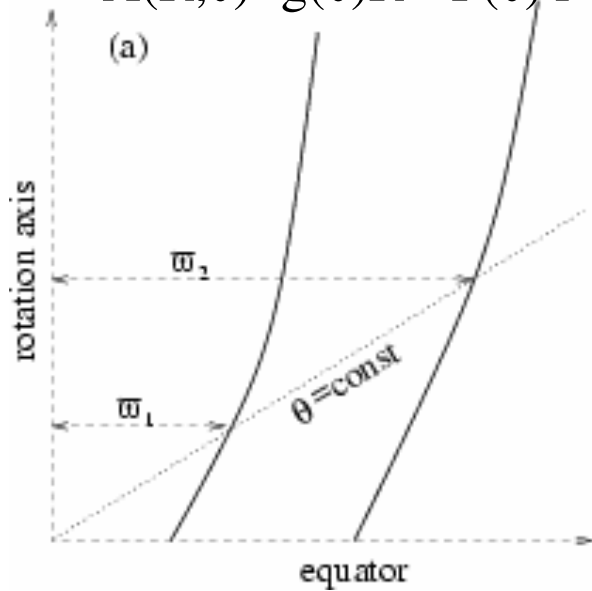
The three classes of exact MHD wind/jet models



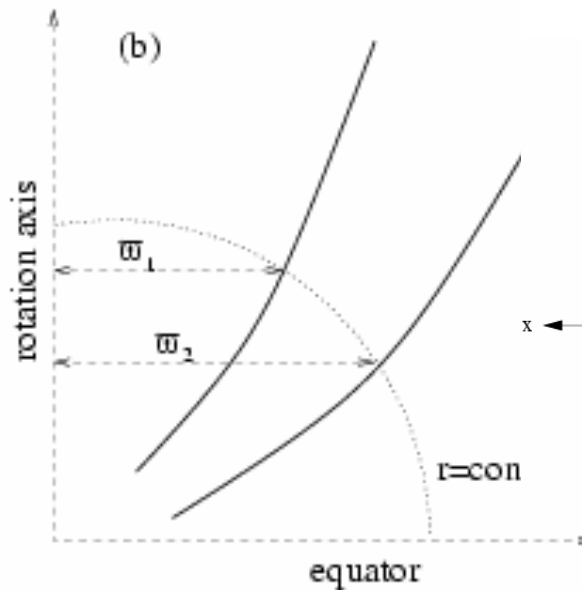
Coronal loop observed with TRACE 26 September 2000

$$r = R \sin \theta$$

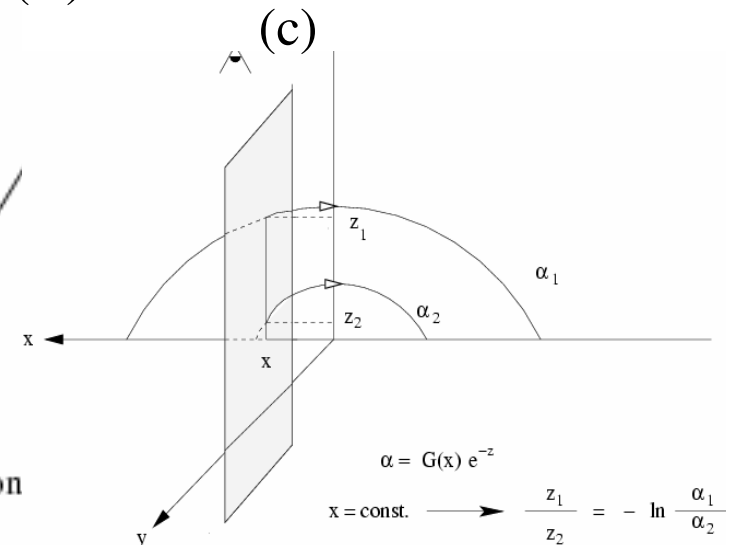
$$A(R, \theta) = g(\theta) R^x = F(\theta) r^x$$



$$A(R, \theta) = f(R) \sin^{2\epsilon} \theta = G(R) r^2$$



$$A(x, z) = G(x) e^{-z}$$



The problem of a **systematic** construction of exact models for astrophysical MHD plasma flows

Cases of exact, self-consistent solutions, studied so far :

- (i) *Cylindrical* self-similarity, $A = f(\varpi)g(z)$:
Chan & Henriksen, 1980, Ap.J, **241**, 534
- (ii) *Radial* self-similarity, $A = f(\theta)r^x$:
($x=3/4$: Blandford & Payne, 1982, MNRAS, **199**, 883)
($x \neq 3/4$: Contopoulos & Lovelace 1994, ApJ, **429**, 139)
($x \neq 3/4$: Vlahakis et al 2000, MNRAS, **318**, 417)
- (iii) *Meridional* self-similarity, $A = f(r)\sin^{2\epsilon}\theta$:
($\epsilon \neq 1$: Lima, Priest & Tsinganos, 2001, A&A, **371**, 240)
($\epsilon=1$: Sauty, Trussoni & Tsinganos 1994, 1997, 1999, 2002, A&A)
- (iv) *Planar* self-similarity, $A = f(x)\exp(-z)$:
(Petrie, Vlahakis & Tsinganos, 2002, A&A, **382**, 1081)
- (v) *General* self-similarity– a unification scheme for all cases :
Vlahakis & Tsinganos, 1998, MNRAS, **298**, 777

In self-similarity, if we know one poloidal streamline we can construct the others. But in order to be able to construct one poloidal streamline, need to calculate $f(\theta)$, or $f(r)$. This is achieved by requiring that the solution pass through appropriate critical points where are found the so-called limiting characteristics, the event horizons of MHD.

Classes of self-similar solutions [Vlahakis+Tsinganos, 298, 777, 1998] :

Meridionally self-similar outflows

Case	$g_1(\alpha)$	$g_2(\alpha)$	$g_3(\alpha)$	
(1)	α	$\lambda^2 \alpha$	$1 + \delta \alpha$	$\leftarrow \lambda=0, \delta=0$: Parker wind
(2)	α	$\xi \alpha + \mu \alpha^\epsilon / \epsilon$	$1 + \delta \alpha + \mu \delta_0 \alpha^\epsilon$	\leftarrow Sauty+kT (1984 - 2004)
(3)	α	$\xi \alpha + \mu \alpha \ln \alpha$	$1 + \delta \alpha + \mu \delta_0 \alpha \ln \alpha$	\leftarrow Lima et al (1986)
(4)	$\alpha_0 e^{\frac{\alpha}{\alpha_0}}$	$\lambda e^{\frac{\alpha}{\alpha_0}}$	$1 + \delta \alpha e^{\frac{\alpha}{\alpha_0}} + \mu \left(e^{\frac{\alpha}{\alpha_0}} - 1 \right)$	
(5)	$\frac{\alpha_0}{\epsilon} \left \frac{\alpha}{\alpha_0} - 1 \right ^{\epsilon-1} \left(\frac{\alpha}{\alpha_0} - 1 \right)$	$\xi \left \frac{\alpha}{\alpha_0} - 1 \right ^\epsilon$	$1 + \delta \left \frac{\alpha}{\alpha_0} - 1 \right ^\epsilon + \mu \left \frac{\alpha}{\alpha_0} - 1 \right ^{\epsilon-1} - \delta - \mu$	
(6)	$-\alpha_0 \ln \left \frac{\alpha}{\alpha_0} - 1 \right $	$\xi \ln \left \frac{\alpha}{\alpha_0} - 1 \right $	$1 + \delta \ln \left \frac{\alpha}{\alpha_0} - 1 \right + \mu \frac{\alpha}{\alpha_0 (\alpha - \alpha_0)}$	
(7)	$\frac{\alpha}{1-\alpha_0}$	$\mu \ln \frac{\alpha}{\alpha_0} + \xi \alpha$	$1 + \delta (\alpha - \alpha_0) + \mu \delta_0 \ln \frac{\alpha}{\alpha_0}$	
(8)	$\frac{\alpha_0}{\epsilon(1-\alpha_0)} \left(\frac{\alpha}{\alpha_0} \right)^\epsilon$	$\lambda_1 \alpha^\epsilon + \lambda_2 \alpha^{\epsilon-1}$	$1 + \delta_1 (\alpha^\epsilon - \alpha_0^\epsilon) + \delta_2 (\alpha^{\epsilon-1} - \alpha_0^{\epsilon-1})$	
(9)	$\frac{\alpha_0}{1-\alpha_0} \ln \frac{\alpha}{\alpha_0}$	$\lambda_1 \ln \frac{\alpha}{\alpha_0} + \frac{\lambda_2}{\alpha}$	$1 + \delta_1 \ln \frac{\alpha}{\alpha_0} + \delta_2 \left(\frac{1}{\alpha} - \frac{1}{\alpha_0} \right)$	

Radially self-similar outflows

Case	$q_1(\alpha)$	$q_2(\alpha)$	$q_3(\alpha)$	
(1)	$\frac{E_1}{F-2} \alpha^{F-2}$	$\frac{D_1}{F-2} \alpha^{F-2}$	$\frac{C_1}{F-2} \alpha^{F-2}$	$\leftarrow F=3/4$: Blandford & Payne (1982)
(2)	$E_1 \ln \alpha$	$D_1 \ln \alpha$	$C_1 \ln \alpha$	
(3)	$E_1 \alpha^{x_1} + E_2 \alpha^{x_2}$	$D_1 \alpha^{x_1} + D_2 \alpha^{x_2}$	$C_1 \alpha^{x_1} + C_2 \alpha^{x_2}$	
(4)	$E_1 \ln \alpha + E_2 \alpha^x$	$D_1 \ln \alpha + D_2 \alpha^x$	$C_1 \ln \alpha + C_2 \alpha^x$	
(5)	$E_1 (\ln \alpha)^2 + E_2 \ln \alpha$	$D_1 (\ln \alpha)^2 + D_2 \ln \alpha$	$C_1 (\ln \alpha)^2 + C_2 \ln \alpha$	
(6)	$E_1 \alpha^x \ln \alpha + E_2 \alpha^x$	$D_1 \alpha^x \ln \alpha + D_2 \alpha^x$	$C_1 \alpha^x \ln \alpha + C_2 \alpha^x$	

The problem of singularities/critical points :

(1) Equation for derivative of poloidal Alfvén number M_a :

$$\frac{dM_a^2}{dR} = \frac{N_M(R, F, M_a; \text{parameters})}{D(R, F, M; \text{parameters})},$$

(2) Equation for derivative of thermal pressure P_0 :

$$\frac{dP_0}{dR} = \frac{N_P(R, F, M_a; \text{parameters})}{D(R, F, M; \text{parameters})},$$

(3) Equation for derivative of expansion function, or P_1 :

$$\frac{dF}{dR} = \frac{N_F(R, F, M_a; \text{parameters})}{D(R, F, M; \text{parameters})},$$

Difficulty: A physically accepted solution is determined by the requirement that it should pass through critical points which are not known *a priori* but are only determined simultaneously with the complete solution !

Singularities (Critical Points) : $N_M = N_F = N_P = D = 0$.

(a) Alfvén transition (star-type singularity): $M_a = 1$

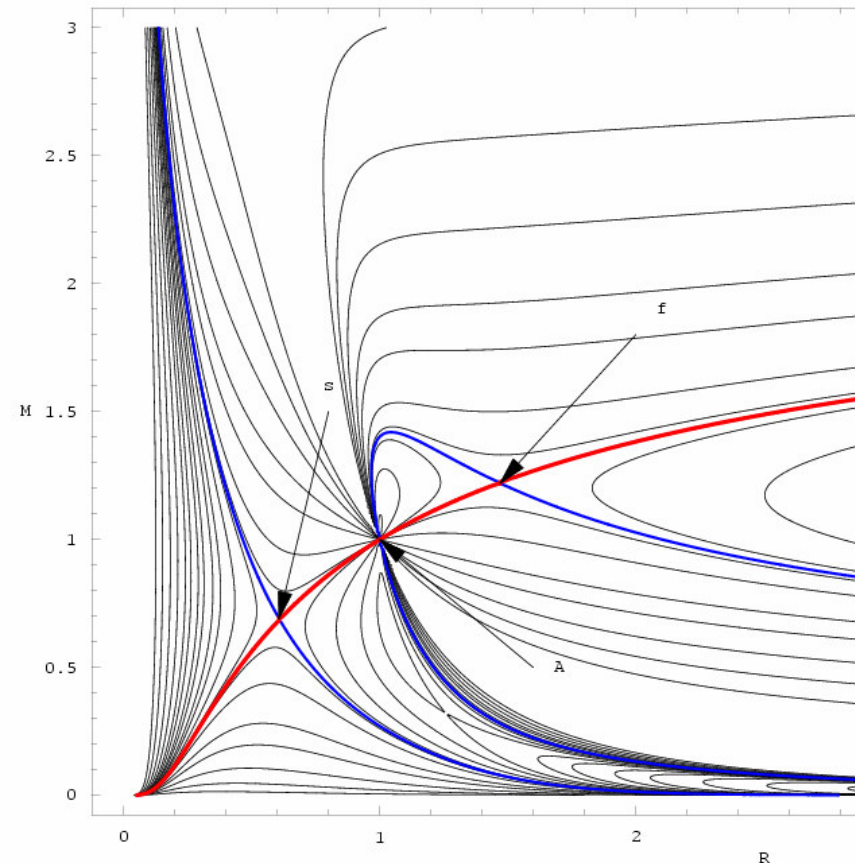
imposes regularity condition \iff streamlines avoid kink.

(b) X-type MHD singularities selecting physical solution
(a proxy for the imposition of physical b.c.'s at r_o and ∞).

\implies Obtain unique solution through critical points.

BUT

at which speeds are found these MHD saddle-type critical points ?



Nature of MHD PDE's & correct boundary conditions

1. *Elliptic* PDE's :

$$\left(\frac{\partial^2 \Phi}{\partial x^2} + \frac{\partial^2 \Phi}{\partial y^2} = 0 \right)$$

⇒ *Dirichlet or Neumann* B.C.'s on a closed surface

2. *Hyperbolic* PDE's :

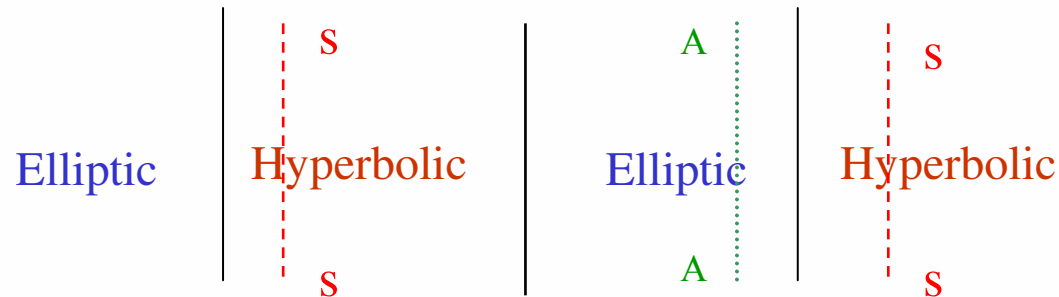
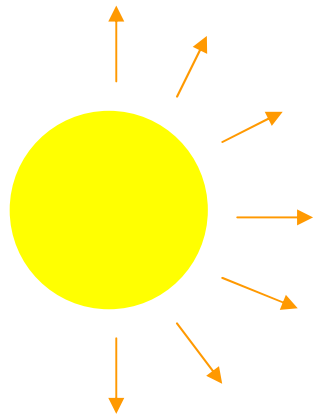
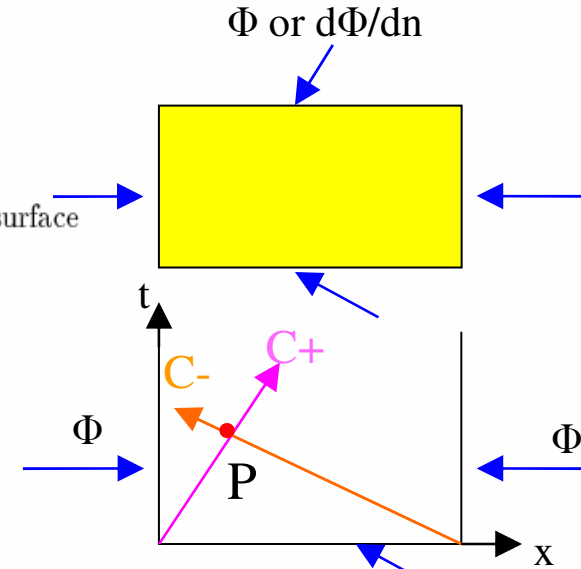
$$\left(\frac{\partial^2 \Phi}{\partial x^2} - \frac{1}{c^2} \frac{\partial^2 \Phi}{\partial t^2} = 0 \right)$$

⇒ *Cauchy* B.C.'s on an open surface.

3. *Mixed Elliptic/Hyperbolic* PDE's :

$$\left[\frac{1 - M_a^2}{h_3^2} \right] \left[\nabla^2 A - \frac{\vec{\nabla} A \cdot \vec{\nabla}(\vec{\nabla} A)^2}{2(\vec{\nabla} A)^2} \frac{V_p^4}{V_p^4 - V_p^2(C_s^2 + V_a^2) + C_s^2 V_{ap}^2} \right] \Phi \text{ and } d\Phi/dt = F_o$$

Elliptic in domains E_i , hyperbolic in domains H_i , $i=1,2, \dots$



⇒ B.C.'s on separatrices SS' in hyperbolic domains H_i .

But, these separatrices SS' in domains H_i are not known *a priori* but should be constructed simultaneously with solution.

The problem of causality and limiting characteristics:

The set of steady MHD equations are of mixed **elliptic/hyperbolic** character.

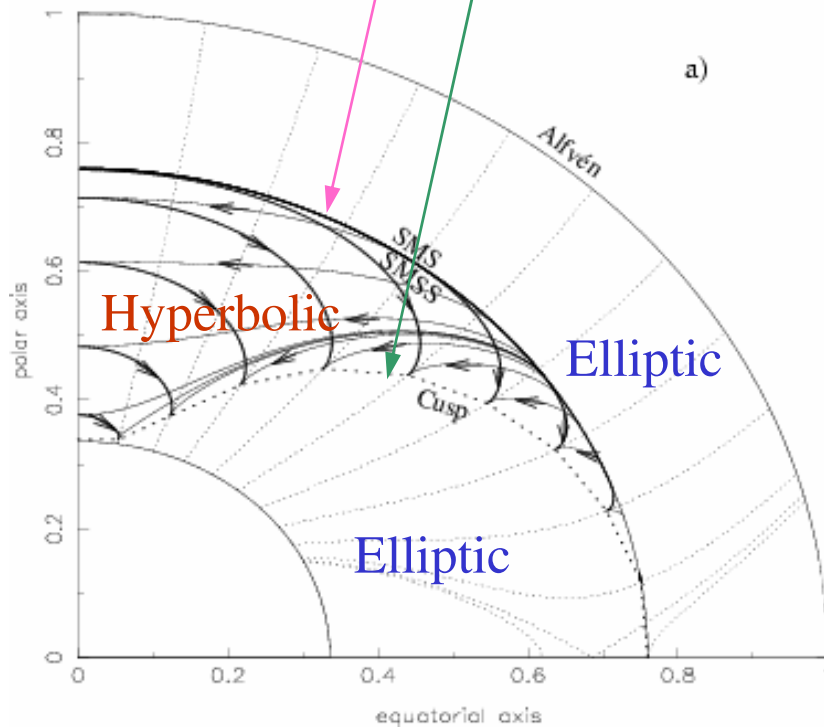
In hyperbolic regimes exist **separatrices** separating causally areas which cannot communicate with each other via an MHD signal. [They are the analog of the limiting cycles in Van der Pol's nonlinear differential equation, or, the **event horizon in relativity**.]

The MHD critical points appear on these separatrices which do not coincide in general with the fast/slow MHD surfaces. To construct a correct solution we need to know the **limiting characteristics**, but this requires an a priori knowledge of the solution we seek for !

Tsinganos et al, MNRAS, 283, 811, 1996

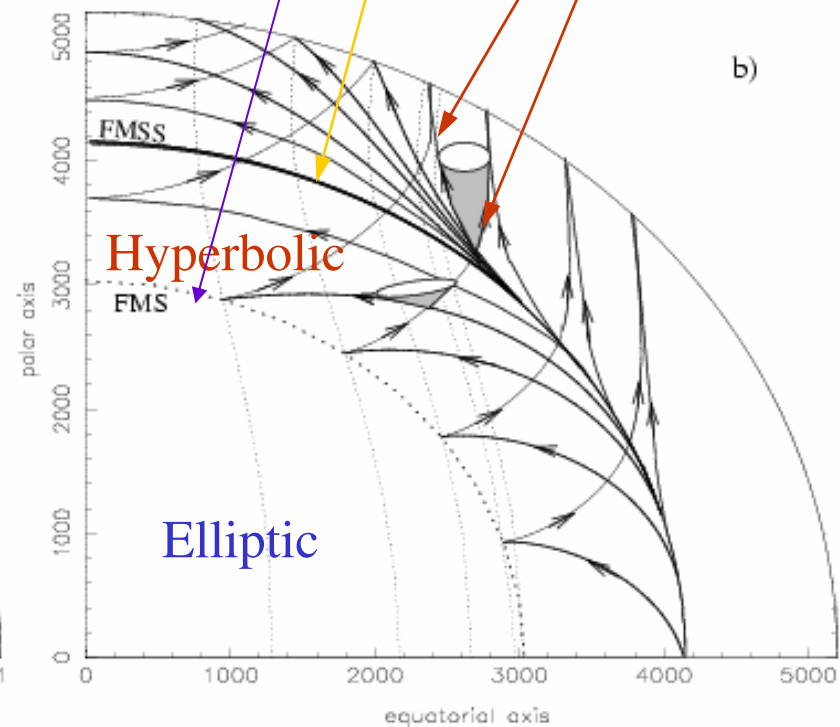
Plot of the characteristics in the 2nd hyperbolic regime of a meridionally self-similar jet.

Dotted lines: poloidal magnetic field lines,
 Solid lines (characteristics)
 Thick-dotted line (cusp surface),
 Dot-dashed line (slow-magnetosonic)

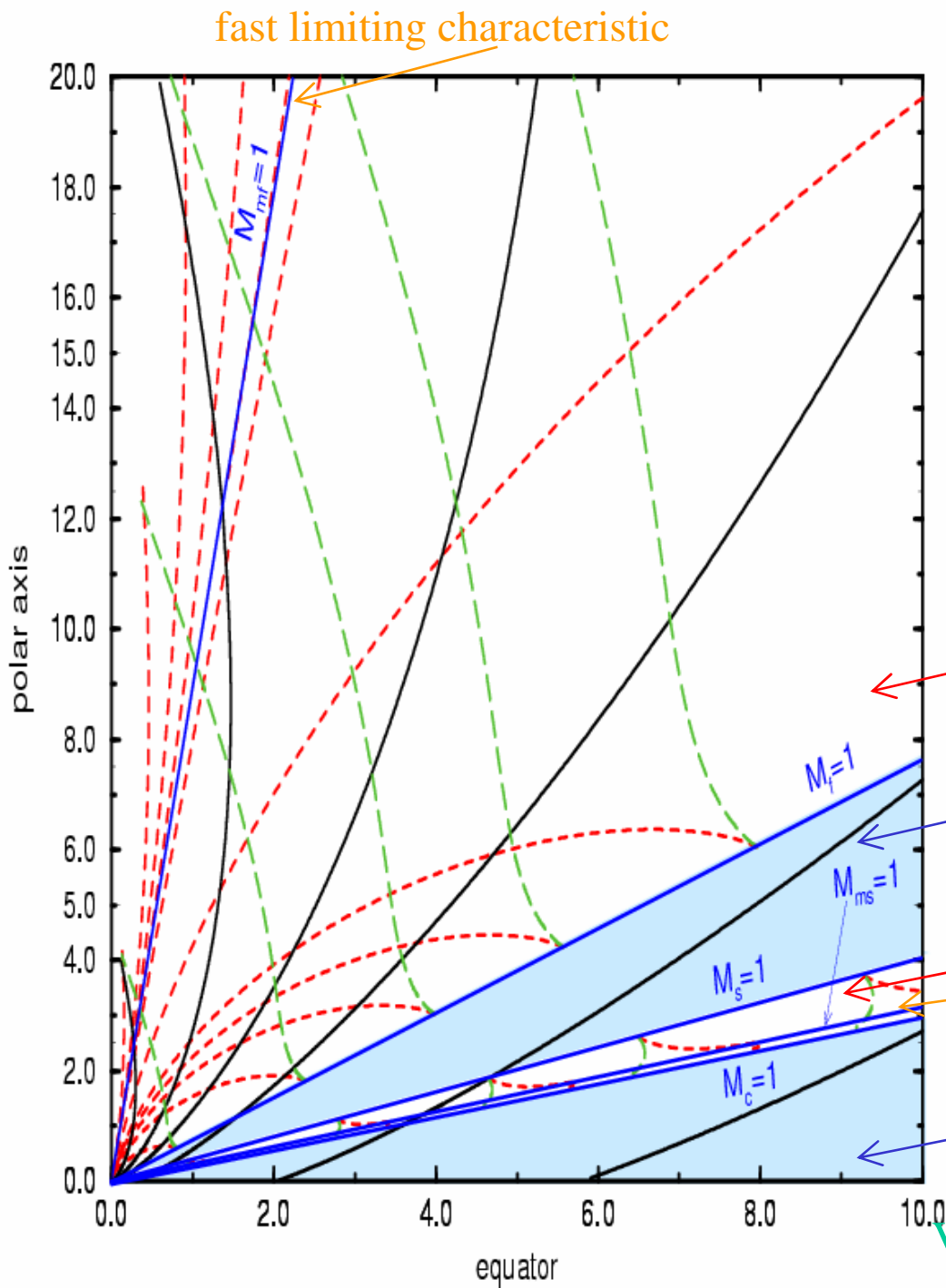


in hyperbolic regime there are two families of characteristics – one of them is tangent to the separatrix-limiting characteristic.

Dotted line (fast-magnetosonic)

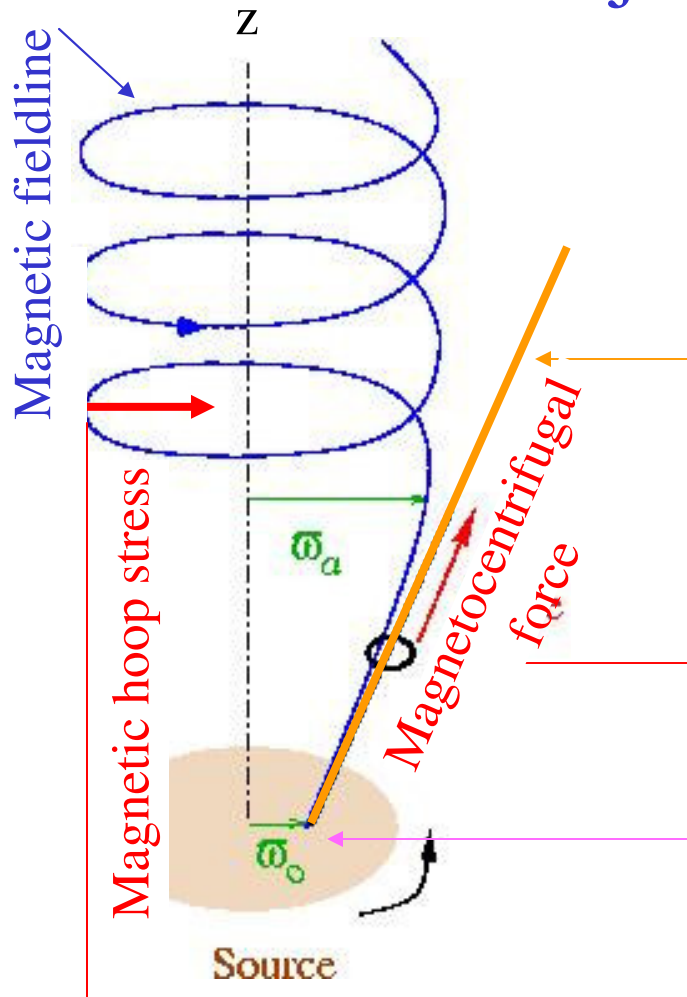


[see Sauty, Trussoni and Tsinganos AA, 421, 797, 2004]



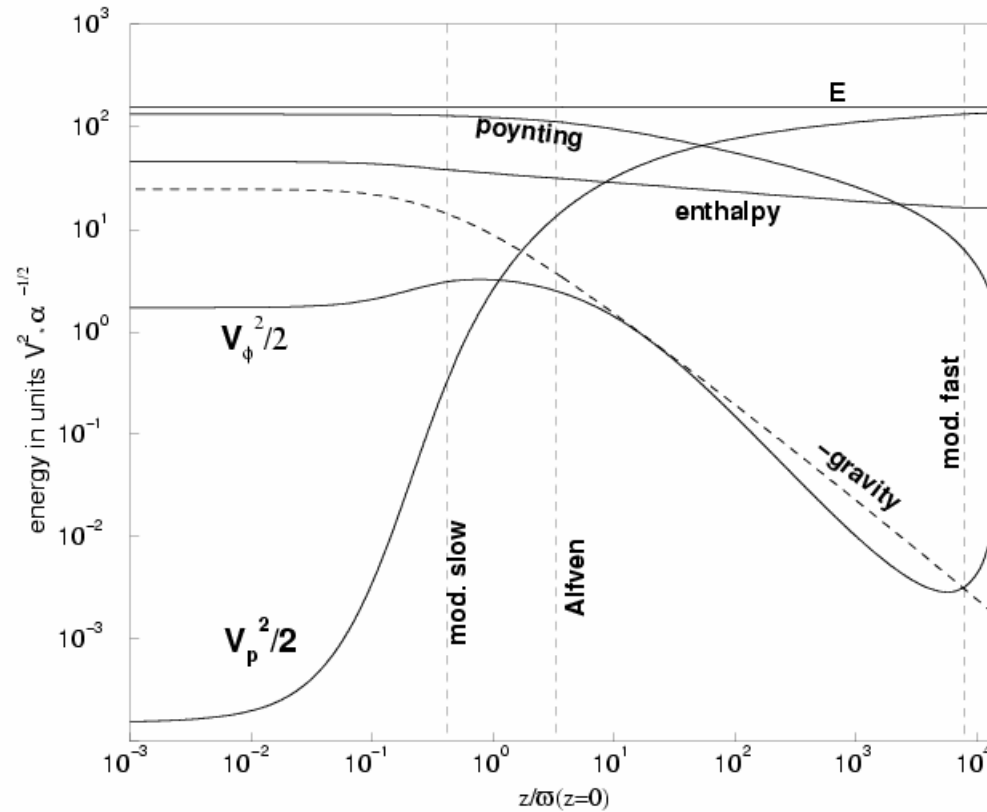
Plot of the characteristics in both hyperbolic regimes of a radially self-similar jet: in each of the two hyperbolic regimes there are two families of characteristics.

Basics of jet acceleration and collimation

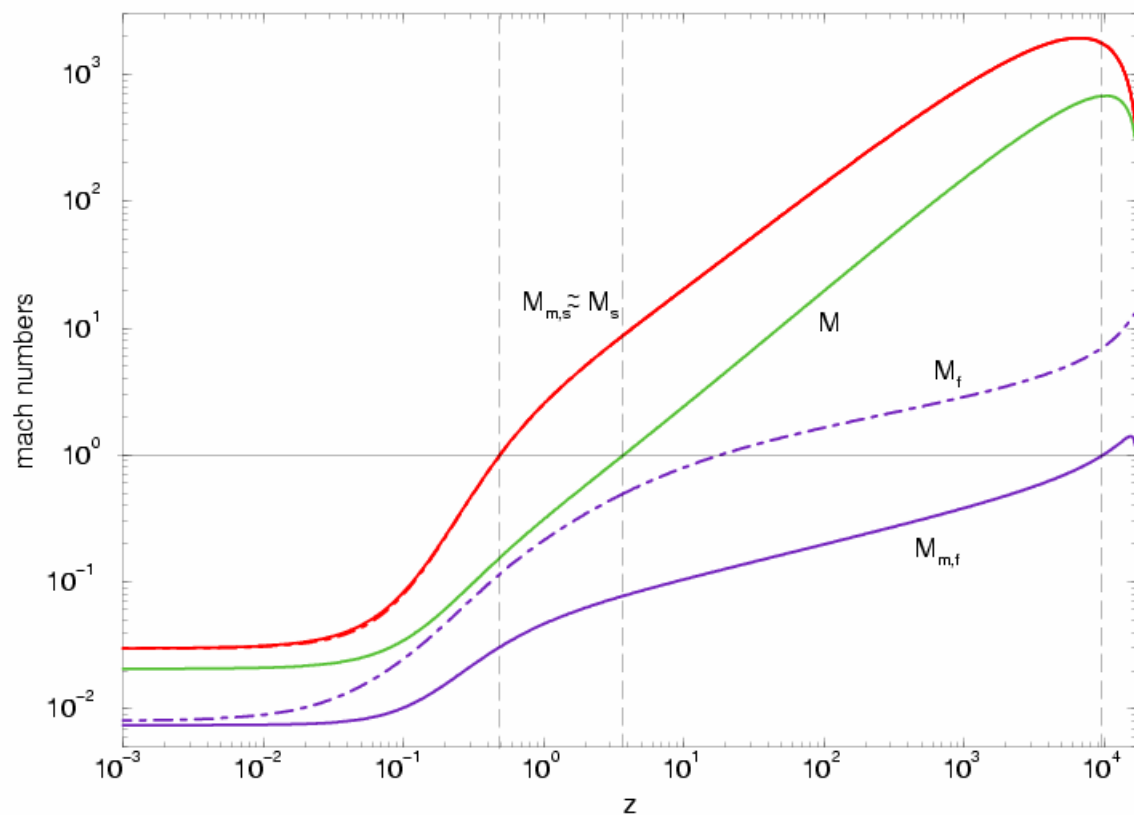


- On the disk, $z=0$, the rotational kinetic energy exceeds the magnetic energy \rightarrow Keplerian rotation of the B-field line rooted at r_0 .
- Up to the Alfvén distance, the B-field is strong enough \rightarrow forces the plasma to follow the Keplerian rotation of the roots of the magnetic fieldline. In particular, when the inclination angle is less than 60° , we have the “bead on a rotating wire” magnetocentrifugal acceleration.
- After the Alfvén distance, the poloidal B-field energy is weaker than the poloidal kinetic motion \rightarrow the B-field follows the plasma. The plasma inertia leaves it behind the rotating B-line \rightarrow creation of strong B_ϕ .
- The created strong B_ϕ collimates the magnetic field lines towards the z-axis and forms the jet.

Poynting driving in magnetocentrifugal disk-winds:



Mach numbers in such magnetocentrifugal disk-winds:



Removal of disk angular momentum by magnetocentrifugal disk-winds:

A Keplerian disk (Ω_K) accreting at a rate \dot{M}_a needs to get rid of angular momentum in a radius ϖ_o :

$$\dot{J}_a = \frac{1}{2} \Omega_K \varpi_o^2 \dot{M}_a$$

A disk-wind carries away angular momentum with a rate :

$$\dot{J}_w = \Omega_K \varpi_A^2 \dot{M}_w$$

If the disk-wind carries away a fraction f ($0 < f < 1$) of the angular momentum of the accreting matter,

$\dot{J}_w = f \dot{J}_a$, then

$$\frac{\dot{M}_w}{\dot{M}_a} = \frac{f \varpi_o^2}{2 \varpi_A^2}$$

With a magnetic lever arm $\varpi \sim 5\varpi_o$, the disk-wind needs to carry away only a few percent of the accreting mass rate.

An energetic criterion for cylindrical collimation:

$$\varepsilon' = \frac{\Delta(\rho E)}{\rho L \Omega}$$

$\Delta f = f(\text{non polar streamline}) - f(\text{polar axis})$

- $\varepsilon' < 0 \rightarrow$ No collimation
- $\varepsilon' > 0 \rightarrow$ Collimation

$$\varepsilon' = \mu + \varepsilon$$

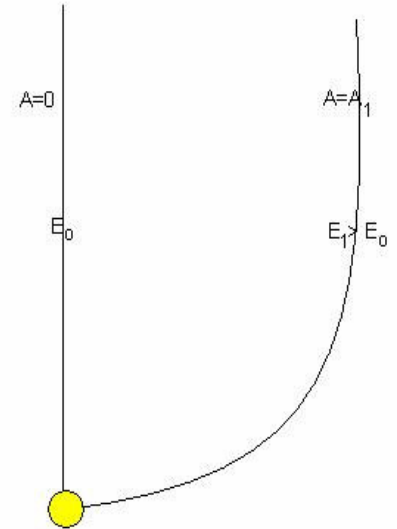
Efficiency of Pressure Confinement

$$\mu \sim \frac{\Delta P}{P} = \kappa$$

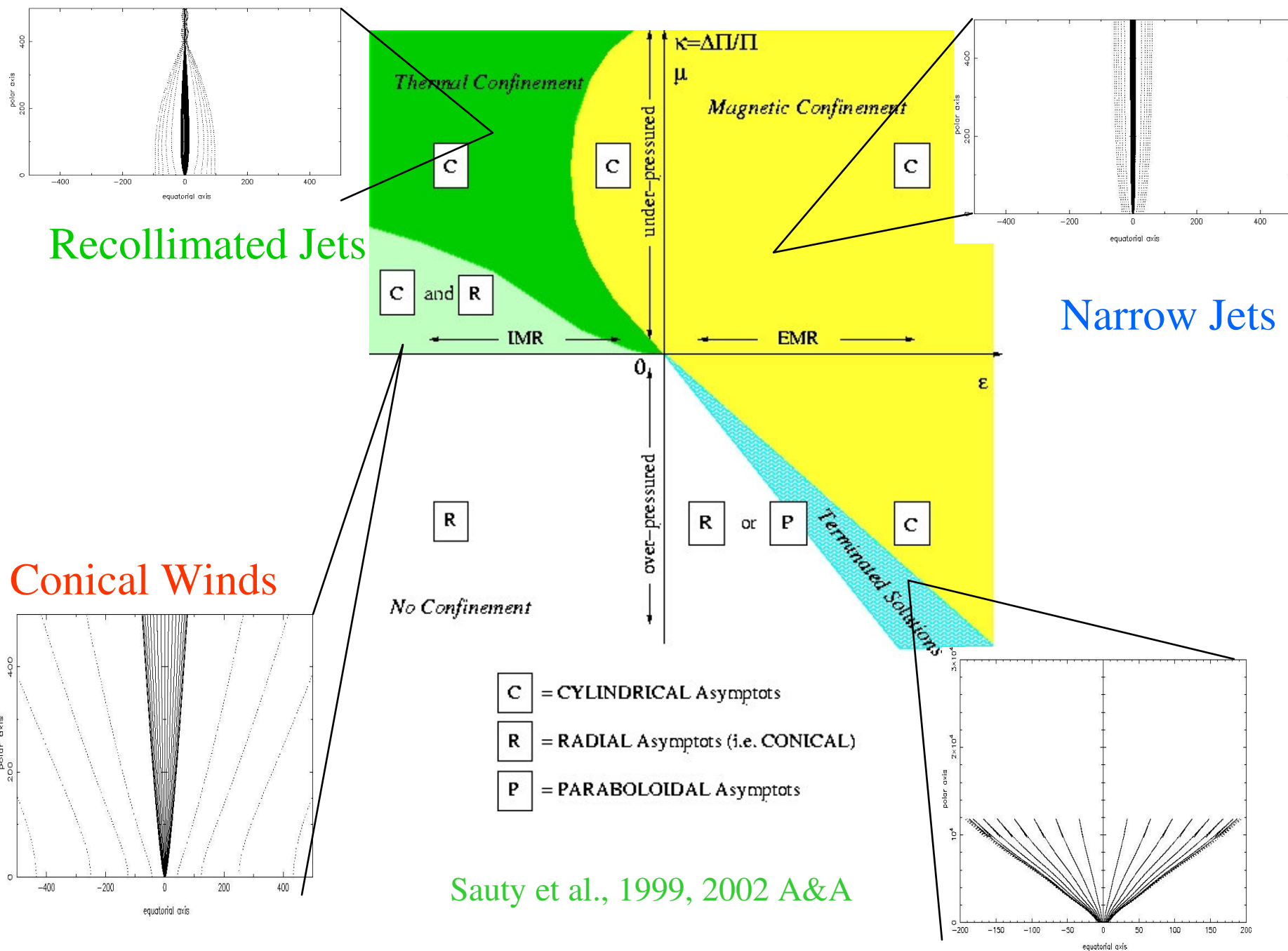
Efficiency of the Magnetic Rotator

$$\varepsilon = \frac{L\Omega - E_{R,o} + \Delta E_G^*}{L\Omega} \quad \text{where} \quad \Delta E_G^* = -\frac{GM}{r_0} \left(\frac{-\Delta T}{T_0} \right)$$

- $\varepsilon > 0 \rightarrow$ Efficient Magnetic Rotator (EMR)
- $\varepsilon < 0 \rightarrow$ Inefficient Magnetic Rotator (IMR)

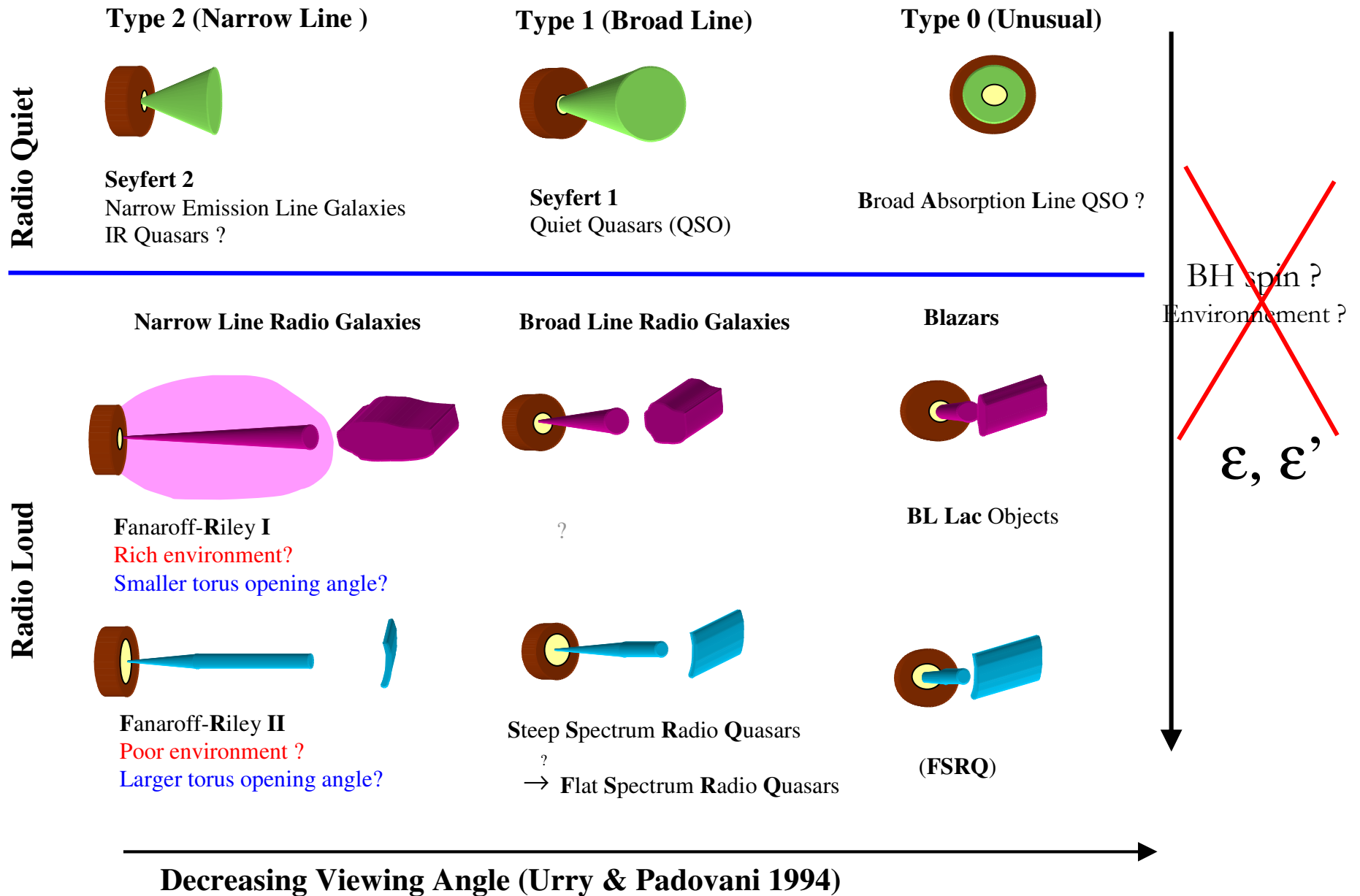


A classification of MHD outflows



Sauty et al., 1999, 2002 A&A

A classification of AGN jets :



But, how general are all those conclusions of the steady exact MHD modelling ?



III) Time-dependent studies

First, demonstration of the formation of a collimated jet once an outflow along a monopole (radial) magnetic field, starts rotating

(jet formation as seen by a naked eye in video).

For details, see :

Bogovalov + Tsinganos, MNRAS, 305, 211, 1999, MNRAS, 325, 249, 2001, MNRAS, 357, 918, 2005

Tsinganos + Bogovalov, AA, 356, 989, 2000, MNRAS, 337, 553, 2002,

Time-dependent MHD equations

$\mathbf{B} = \mathbf{B}_p + \mathbf{B}_\varphi$, $\mathbf{B}_p = \nabla \times \frac{A(z, \varpi, t) \hat{\varphi}}{\varpi}$ Define poloidal magnetic field in terms of vector potential A_φ

$$\frac{\partial A}{\partial t} = -V_\varpi \frac{\partial A}{\partial \varpi} - V_z \frac{\partial A}{\partial z}, \quad \text{Poloidal component of induction equation}$$

$$\frac{\partial \rho}{\partial t} = -\frac{1}{\varpi} \frac{\partial}{\partial \varpi} (\rho \varpi V_\varpi) - \frac{\partial}{\partial z} (\rho V_z), \quad \text{Continuity equation}$$

$$\frac{\partial B_\varphi}{\partial t} = \frac{\partial}{\partial z} (V_\varphi B_z - V_z B_\varphi) - \frac{\partial}{\partial \varpi} (V_\varpi B_\varphi - V_\varphi B_\varpi), \quad \text{Azimuthal component of induction equation}$$

$$\frac{\partial V_\varphi}{\partial t} = -\frac{V_\varpi}{\varpi} \frac{\partial}{\partial \varpi} (\varpi V_\varphi) - V_z \frac{\partial V_\varphi}{\partial z} + \frac{1}{4\pi\rho} \left(B_\varpi \frac{\partial}{\partial \varpi} (\varpi B_\varphi) + B_z \frac{\partial B_\varphi}{\partial z} \right), \quad \text{Azimuthal component of momentum equation}$$

$$\frac{\partial V_z}{\partial t} = -V_\varpi \frac{\partial V_z}{\partial \varpi} - V_z \frac{\partial V_z}{\partial z} - \frac{1}{\rho} \frac{\partial P}{\partial z} - \frac{GMz}{r^3} - \frac{1}{8\pi\rho\varpi^2} \frac{\partial}{\partial z} (\varpi B_\varphi)^2 - \frac{B_\varpi}{4\pi\rho} \left(\frac{\partial B_\varpi}{\partial z} - \frac{\partial B_z}{\partial \varpi} \right), \quad \text{z- component of momentum equation}$$

$$\frac{\partial V_\varpi}{\partial t} = -V_\varpi \frac{\partial V_\varpi}{\partial \varpi} - V_z \frac{\partial V_\varpi}{\partial z} - \frac{1}{\rho} \frac{\partial P}{\partial \varpi} - \frac{GM\varpi}{r^3} - \frac{1}{8\pi\rho\varpi^2} \frac{\partial}{\partial \varpi} (\varpi B_\varphi)^2 + \frac{V_\varphi^2}{\varpi} + \frac{B_z}{4\pi\rho} \left(\frac{\partial B_\varpi}{\partial z} - \frac{\partial B_z}{\partial \varpi} \right), \quad \text{Radial component of momentum equation}$$

$(z, \varpi, \varphi) \Rightarrow$ cylindrical coordinates,

$\rho(z, \varpi, t) \Rightarrow$ density,

$\vec{V}(z, \varpi, t) \Rightarrow$ flow speed,

$\vec{B}(z, \varpi, t) \Rightarrow$ magnetic field,

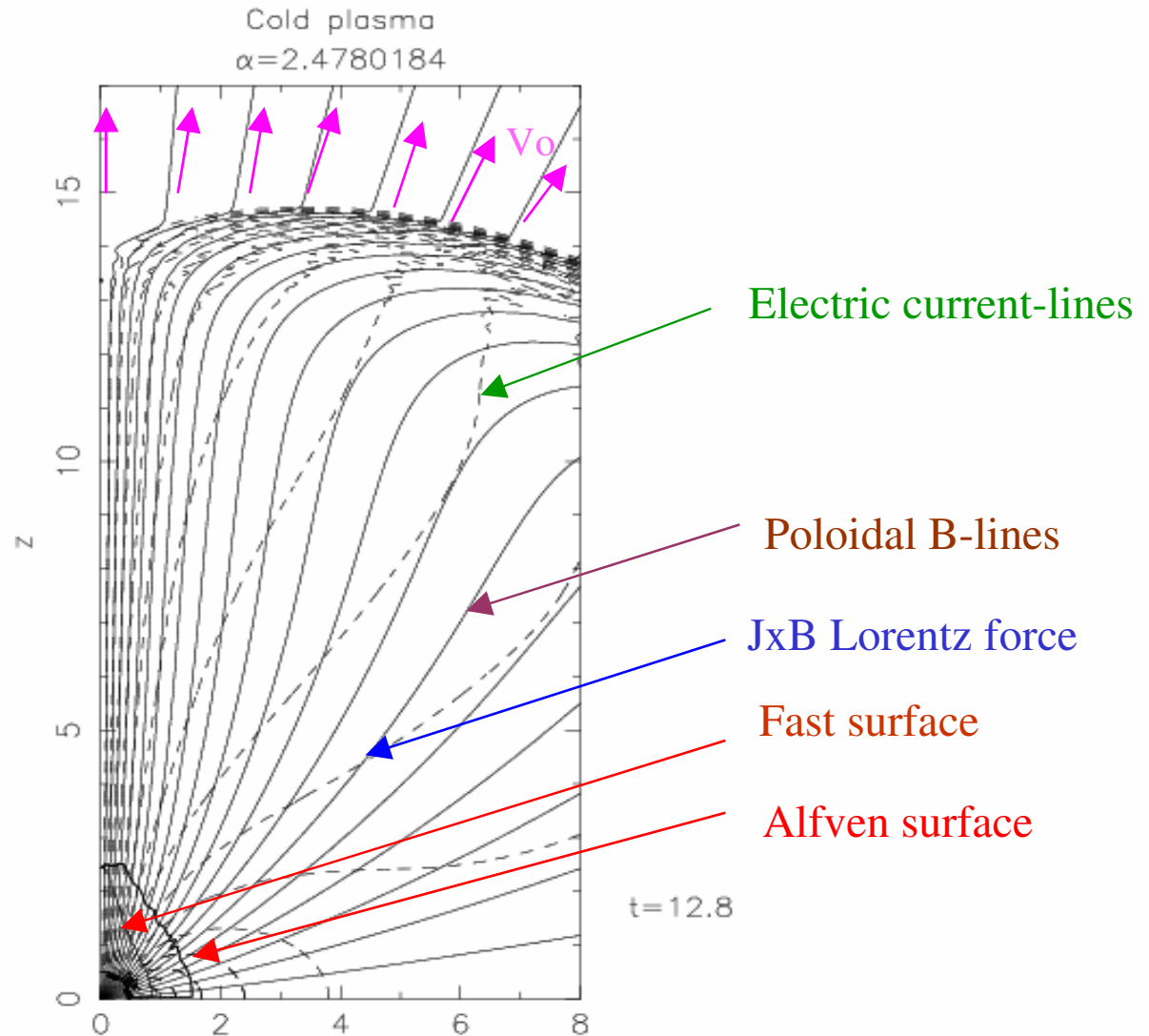
$A(z, \varpi, t) \Rightarrow$ poloidal magnetic flux.

Close system either with **polytropic** equation of state,
or, by adding an **energy** equation.

A near zone snapshot on the poloidal plane showing the change of shape of the poloidal magnetic field from an initially uniform with latitude radial monopole (before a stationary state is reached).

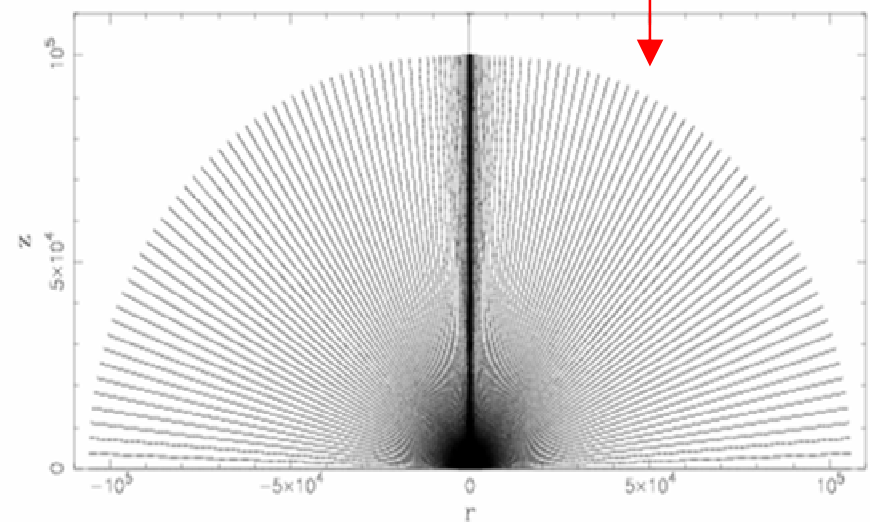
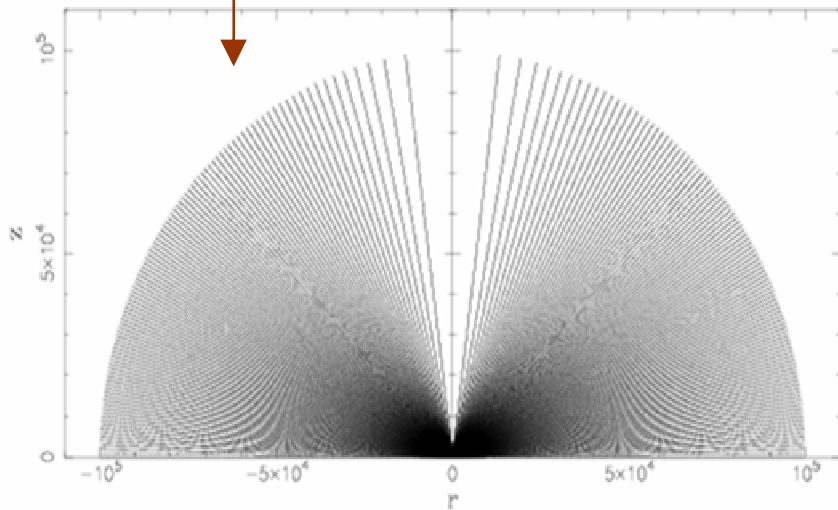
$$\alpha = \frac{\Omega R_a}{V_o} = \frac{2\pi T_{\text{travel}}}{T_{\text{rotation}}}$$

$\alpha < 1$: Slow rotators
 $\alpha > 1$: Fast rotators

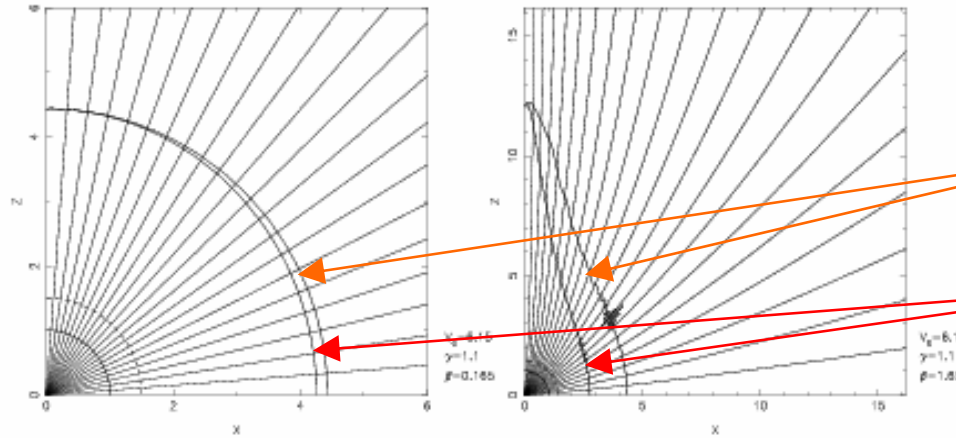


Far Zone :
Poloidal magnetic lines of outflow :
(at intervals of equal magnetic flux)

Before rotation starts – After rotation started



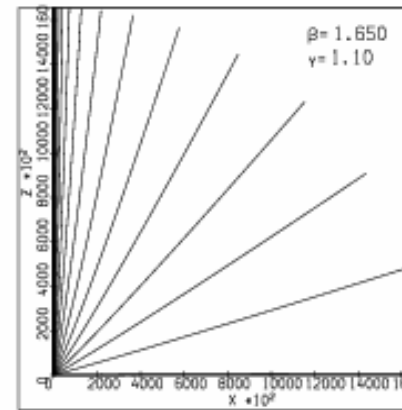
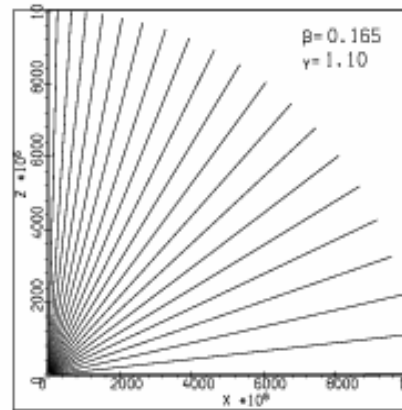
Solution in Near Zone



Fast surface

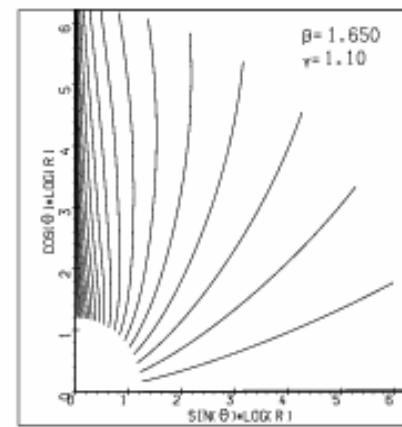
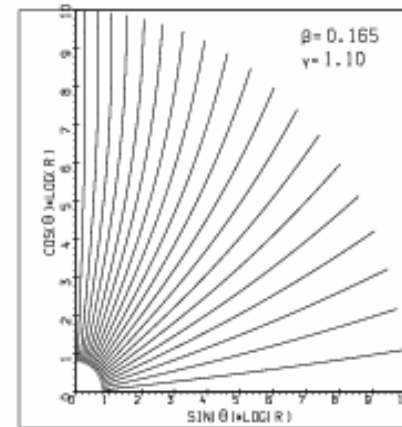
Alfven surface

Weak collimation of outflow from a SLOW magnetic rotator (e.g., our Sun)



Strong collimation of outflow from a FAST magnetic rotator (e.g., a 10 times faster rotating YSO)

Solution in far zone (Logarithmic Plot !)



Solution in far zone (Logarithmic Plot !)

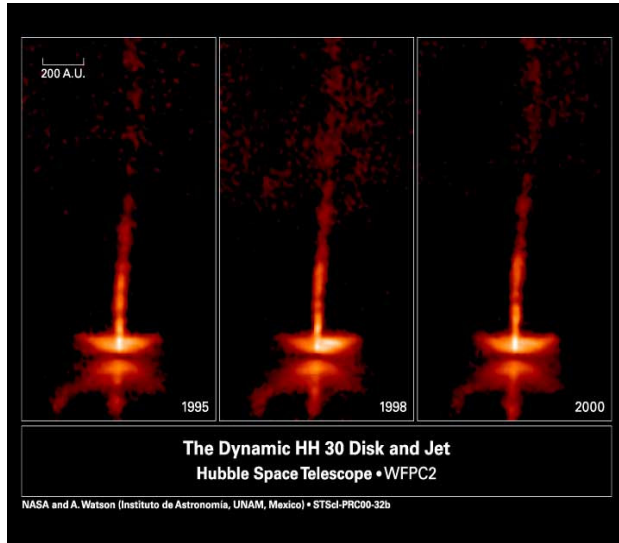


Astrophysical implications: an evolutionary scenario

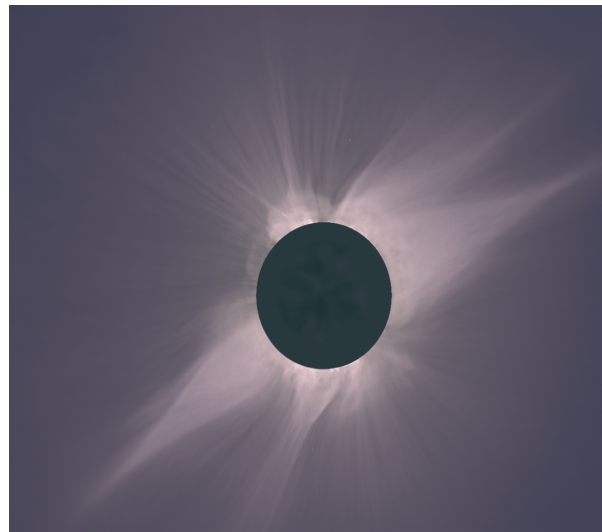
- Start with a non rotating star/disk system having a radial magnetic field.
- As system rotates, poloidal fieldlines focus towards axis by magnetic tension.
- Parameter $\alpha = (\text{corotating speed at Alfvén distance}) / (\text{initial flow speed})$.
- Radius of formed jet $R_{jet} \propto 1/\alpha$.
- Significant flow collimation in fast magnetic rotators with $\alpha > 1$, while very weak collimation in slow magnetic rotators with $\alpha < 1$.
- Reversing time: start with a tightly collimated outflow ($\alpha > 1$) and reduce α to small values, $\alpha \rightarrow 0$:
⇒ sequence analogous to evolution of outflow geometry from a YSO.
- Efficient magnetic rotators have large values of α
⇒ highly collimated jets, as observed in association with YSOs.
- As star ages losing angular momentum it may gradually shift to the stage of a slow magnetic rotator with small α values like our own Sun which produces the almost radial outflow of the solar wind.
- Scenario agrees very well with results of steady (self-similar) modelling where a quantitative *energetic criterion* is given for separating loosely collimated winds associated with efficient magnetic rotators from tightly collimated jets associated with efficient magnetic rotators.
- For large values of α , the magnitude of the flow speed in the jet remains below the fast MHD wave speed everywhere
⇒ outflows from classical thin accretion disks may rather be nonstationary and turbulent.

The Dichotomy of Winds and Jets

- Jets = tight collimation

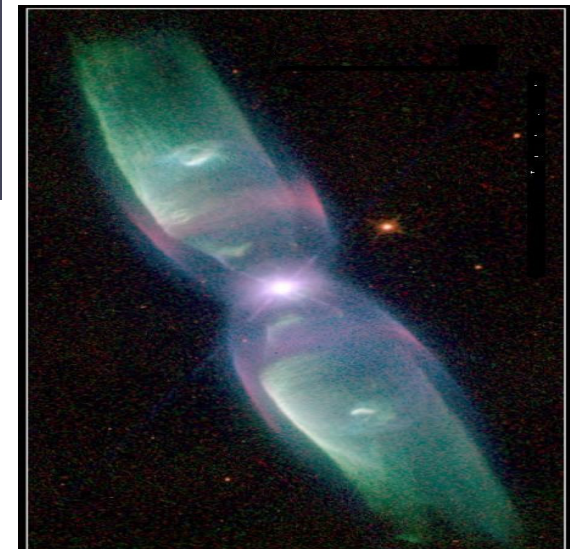


- Winds = no collimation



1. Star-birth (YSO)

2. Solar Wind



3. Star-death (PN)

Stellar Evolution

However, several pbs with 1-component outflows:

Small fraction of mass and magnetic flux is collimated in a single-component outflow.

Weak collimation in case in the central outflow there is no available a strong azimuthal magnetic field, or, the central flow is relativistic (as in AGN jets).

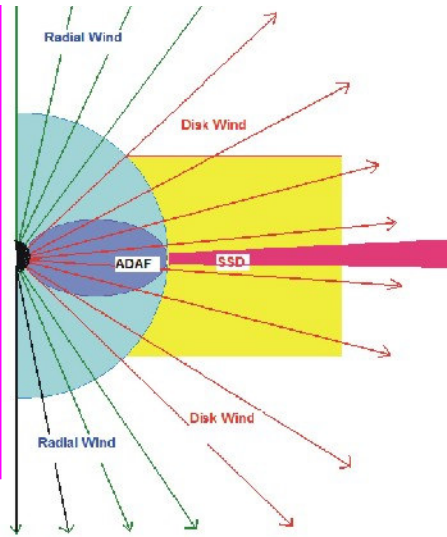
Note also that disk-wind models are “singular” around rotation axis.

A central magnetized wind is needed to slow down the young star

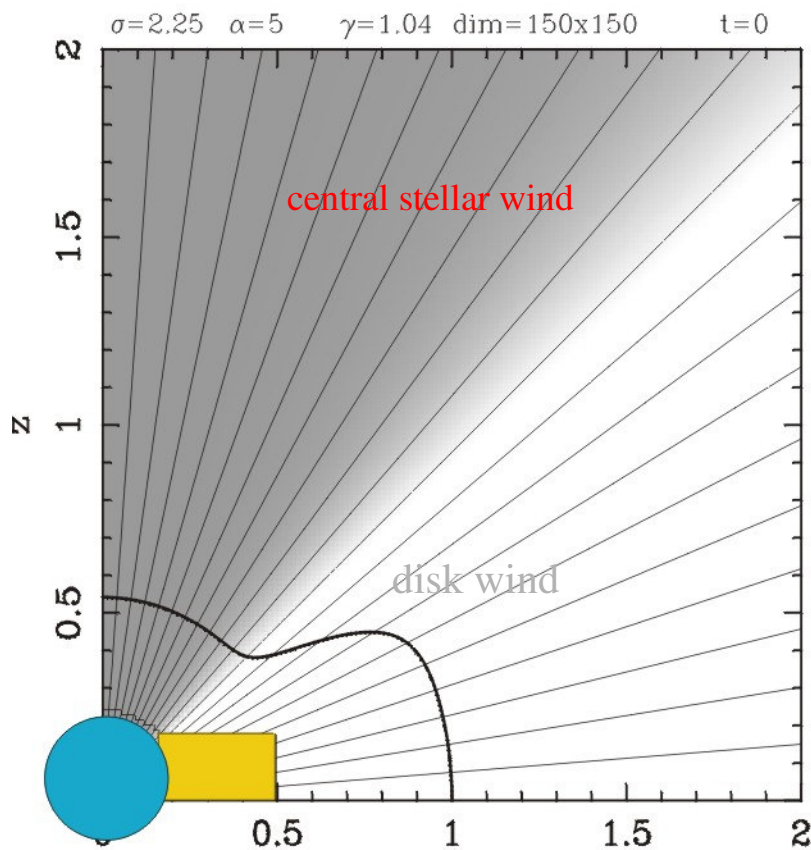
A two-component outflow model with :

a) a central stellar wind

b) a disk-wind

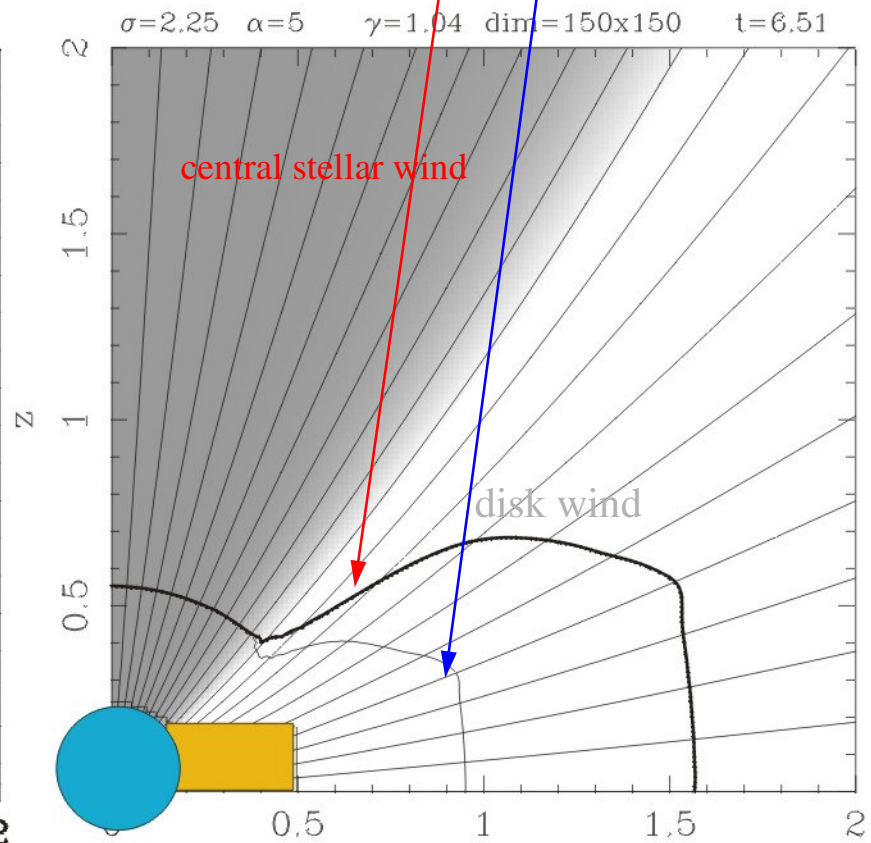


Before rotation starts

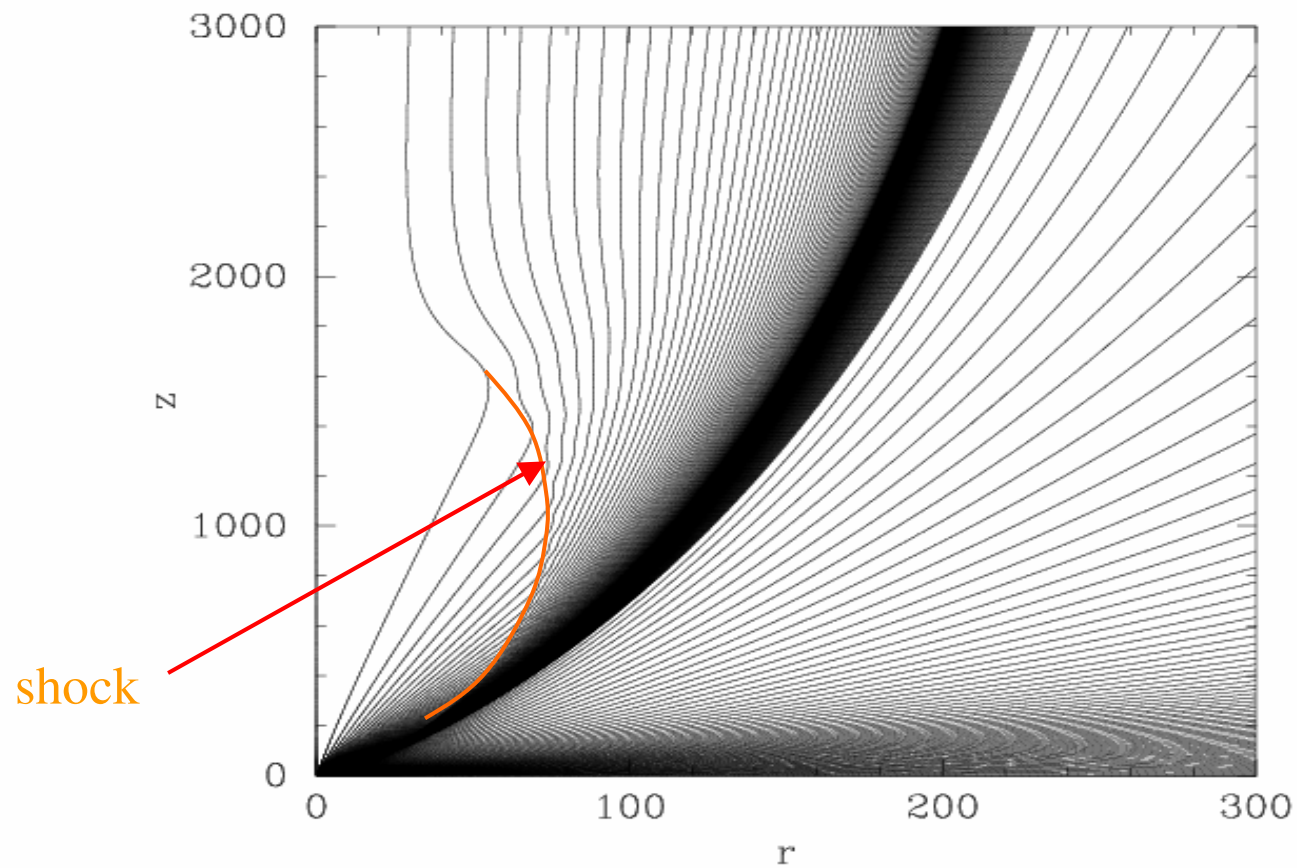


Fast surface
Alfven surface

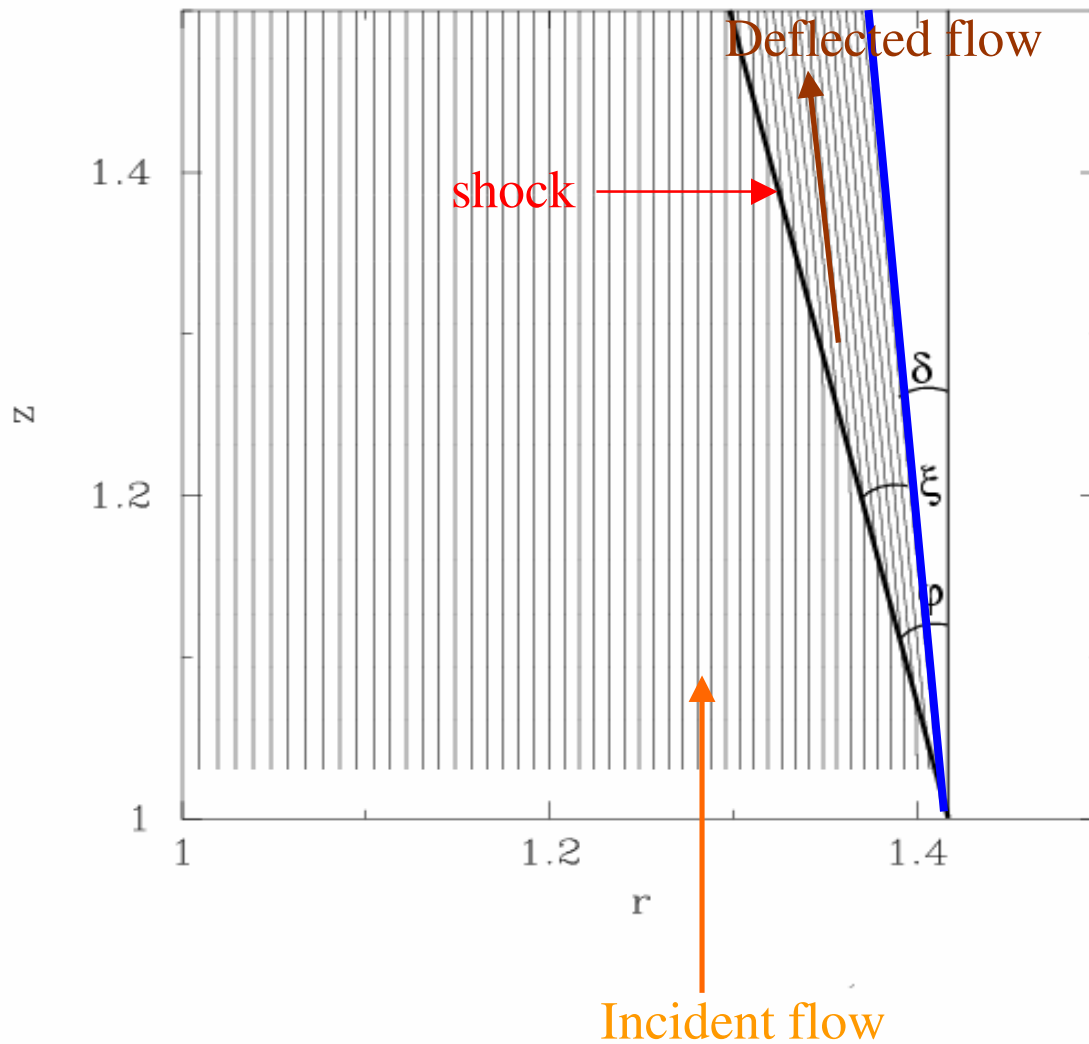
After rotation starts



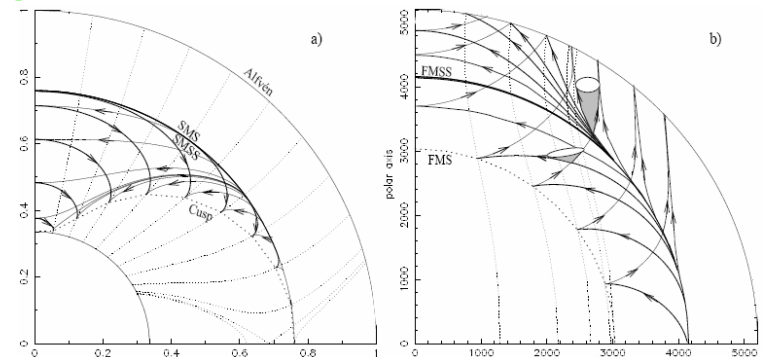
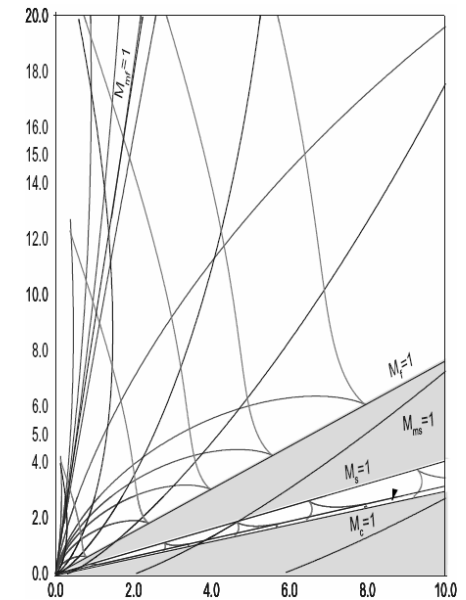
Collimation of the inner flow with the formation of a shock.



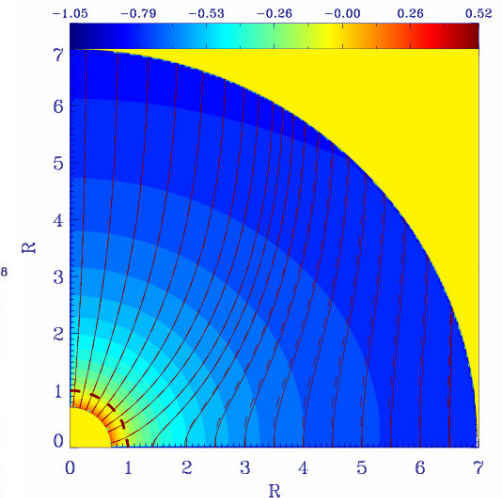
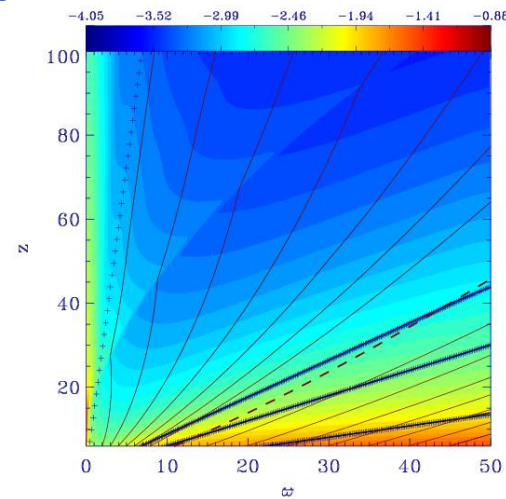
Real-life example: Supersonic flow incident at the vertex of an angle



- **The Radially Self Similar Models (r -ss):**
 - Describe **magneto-centrifugally driven disk winds**
 - They have **conical** critical surfaces
 - Allow **a constant- γ** pressure-density relation
 - However, they are **singular** at the z-axis
- **The Meridionally Self Similar Models (θ -ss):**
 - Describe **thermally driven stellar outflows**
 - Have **spherical** critical surfaces
 - Have **variable** effective polytropic index
 - However, **not all magnetic fieldlines are connected to the stellar surface**

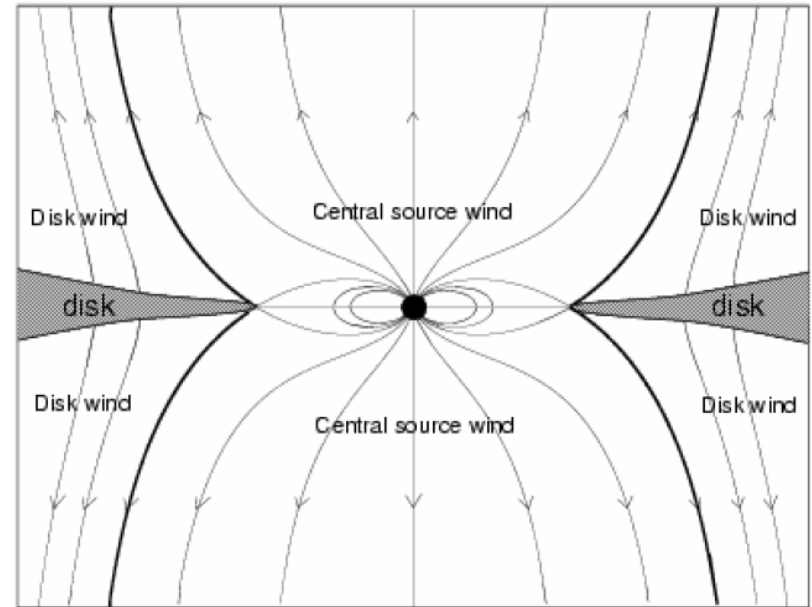


- The two classes of solutions are complementary:
 - Axis (**stellar outflows**) best described by **meridionally** self-similar solutions
 - Equator (**disk winds**) best described by **radially** self-similar solutions



- The first thing is to show the topological stability of the solutions along with other physical and numerical features [Matsakos et al, 2007, A+A in press].

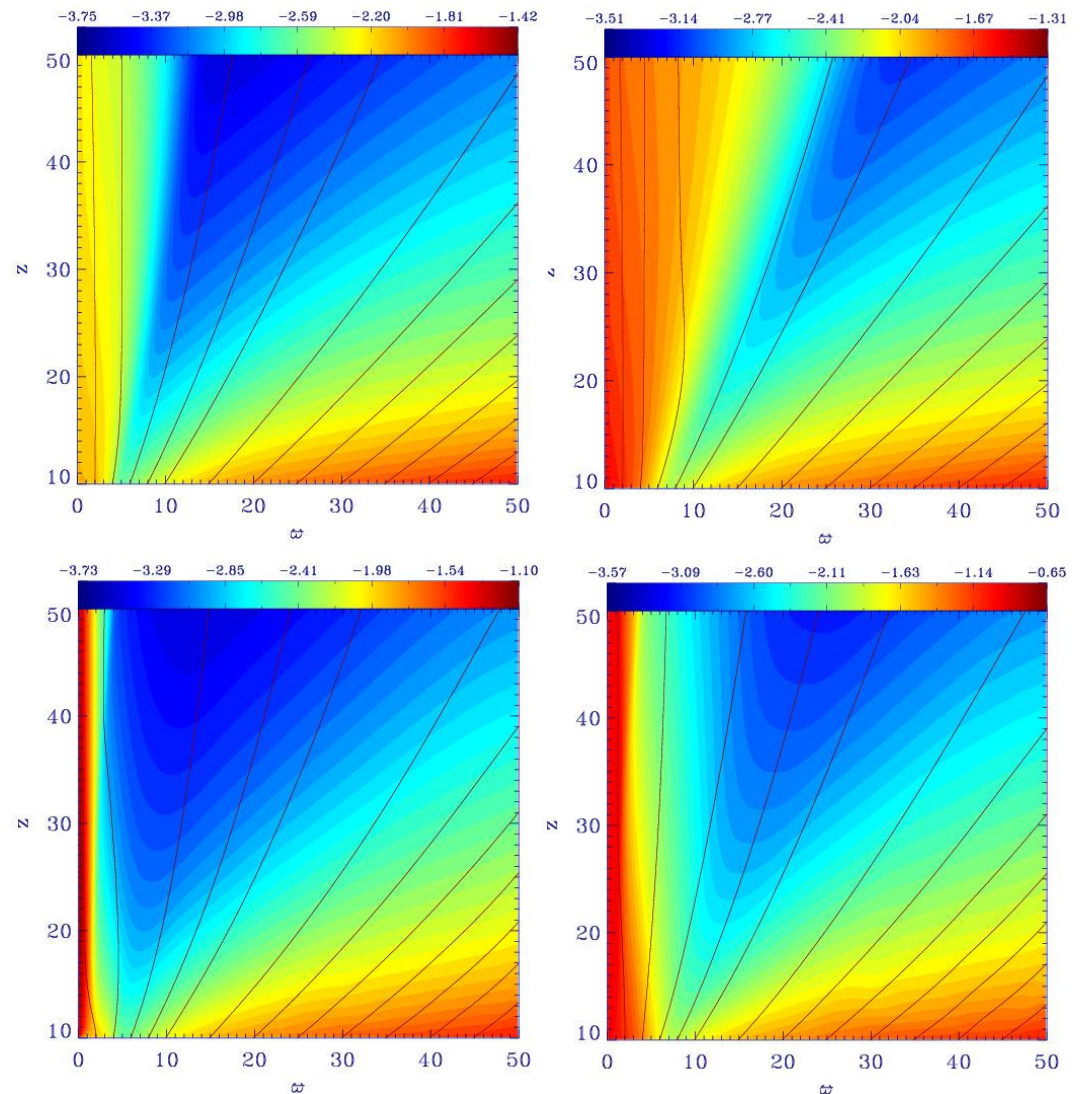
- Choice of contribution in the total magnetic field
- Choice of a fieldline (α_0)
- Choice of the steepness of the transition (d)
- Then, initialize each solution with the mixing function:



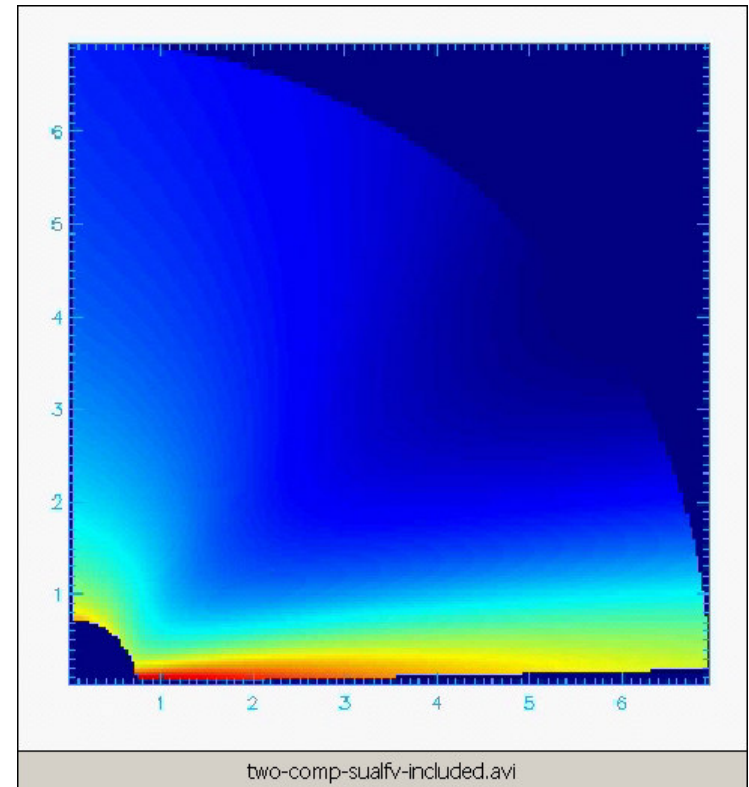
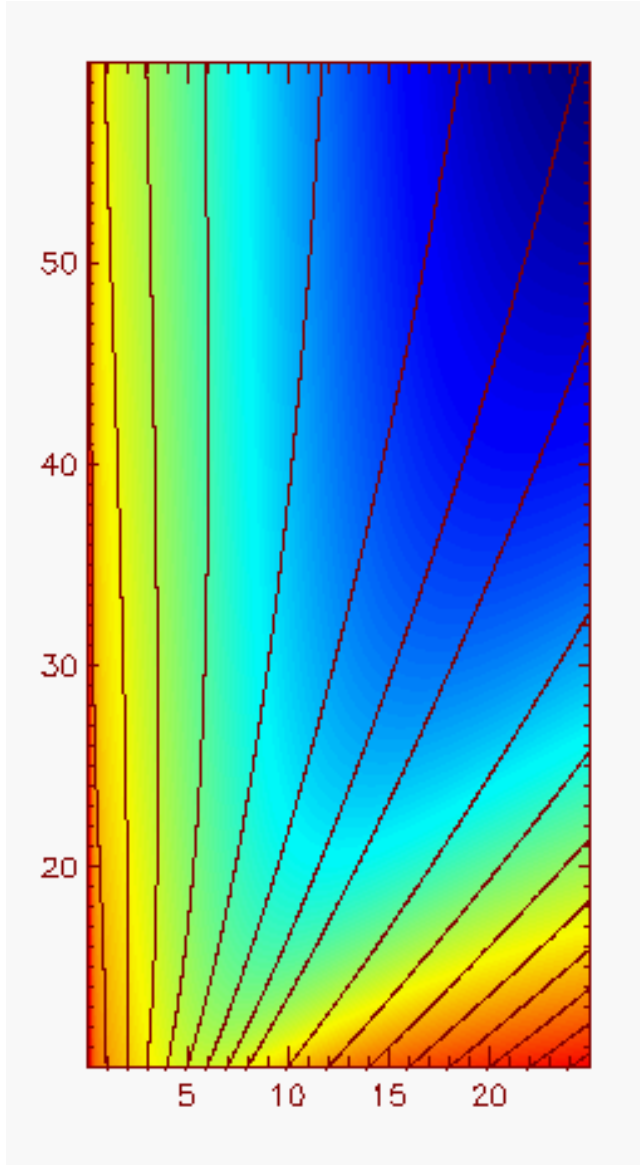
$$V_{2-comp}(\varpi, z) = w_1 V_{\theta ss}(\varpi, z) + w_2 V_{r ss}(\varpi, z)$$

$$w_1 = \exp \left\{ -c \left[\frac{\alpha(\varpi, z)}{\alpha_0} \right]^d \right\} \quad \text{and} \quad w_2 = 1.0 - w_1$$

- **Initial setup:**
 - Implementation of both solutions
 - Different contribution of the stellar wind (left and right)
- **Final setup:**
 - Steady-state reached
 - Disk wind does not change
 - Stellar wind is being collimated by the disk component



Results of evolved 2-component



- A steady-state is always reached, however at different timescales for each model
- The disk wind remains almost unmodified while effectively collimating the inner stellar outflow
- The final outcome of the simulations stays close to the initial setup, hence retaining the validity of the analytical solutions
- Proper choice of the parameters can explain many of the observed cases of the two-component jets i.e. from the one extreme of stellar dominated ones, up to the other, of the disk-wind being the only contributor

Some conclusions

- Systematic analytical construction of classes of exact MHD models for jets
- Critical role played by of limiting characteristics in setting correct BC's
- Energetic criterion for the transition between winds $\leftarrow \rightarrow$ jets
- Topological stability of most analytical MHD jet models
- Time-dependent simulations support general trends of exact steady studies
- A new 2-component model is needed to describe collimated outflows
- There is yet a new way for producing shocks in jets